Electronic Supplementary Information (ESI) for

Forcing single-chain nanoparticle collapse through hydrophobic solvent interactions in comb copolymers

Cheyenne H. Liu, Logan D. Dugas, Jared I. Bowman, Tamuka Chidanguro, Robson F. Storey and Yoan C. Simon*

School of Polymer Science and Engineering, The University of Southern Mississippi, 118 College Drive #5050, Hattiesburg MS 39406, United States.

*To whom correspondence should be addressed. email: yoan.simon@usm.edu

Contents

Experimental

I. Materials and Instrumentation

All reagents were obtained from commercial sources and used as received unless otherwise noted. Grubbs' second-generation catalyst [$(H_2IMes)(PCy_3)(Cl)_2Ru$=CHPh] was purchased from AK Scientific, and Grubbs' third-generation catalyst (G3) was prepared in a glovebox according to the reported procedure.[1] CH_2Cl_2 was dried by distillation and stored over molecular sieves. Deuterated solvents were purchased from Sigma Aldrich and used as received.

^{1}H nuclear magnetic resonance (^{1}H NMR) spectroscopy

Nuclear magnetic resonance experiments were performed with either a Varian MERCURY^{plus} 300 MHz (VNMR 6.1C) or a Bruker AVANCE III 600 MHz (TopSpin 3.1) spectrometer.

^{13}C nuclear magnetic resonance (^{13}C NMR) spectroscopy

Nuclear magnetic resonance experiments were performed with a Bruker AVANCE III 600 MHz (TopSpin 3.1) spectrometer.

Size-exclusion chromatography (SEC)

SEC was conducted using a Waters Alliance 2695 separations module, an online multiangle laser light scattering (MALLS) detector fitted with a gallium arsenide laser (20 mW) operating at 658 nm (miniDAWN TREOS, Wyatt Technology Inc.), an interferometric refractometer (Optilab T-rEX, Wyatt Technology Inc) operating at 35 °C, and 685 nm, and two PLgel mixed E columns (Polymer Laboratories Inc.) in series (pore size 50-10^3 Å, 5 μm bead size). The mobile phase was freshly distilled THF delivered at a flow rate of 1.0 mL/min. Sample concentrations were 2.5 mg of polymer/mL of THF, and the injection volume was 100 μL. The detector signals were simultaneously recorded using ASTRA software (Wyatt Technology, Inc.), and absolute molecular weights were determined by MALLS using a *dn/dc* value obtained from the interferometric refractometer response and assuming 100% mass recovery from the columns.

Matrix-assisted laser desorption/ionization time-of-flight mass spectrometry (MALDI-TOF MS)

Matrix-assisted laser desorption/ionization time-of-flight mass spectrometry (MALDI-TOF MS) was performed using a Bruker Microflex LRF MALDI-TOF mass spectrometer equipped with a nitrogen laser (337 nm) possessing a 60 Hz repetition rate and 42.5 μJ energy output. The PIB samples were prepared using the dried droplet method: separately prepared THF solutions of DCTB matrix (20 mg·mL^{-1}), oNBMIPIB sample (10 mg·mL^{-1}), and AgTFA cationizing agent (10 mg/mL) were mixed in a volumetric ratio of matrix/sample/cationizing agent = 8:1:0.2, and a 0.5 μL aliquot was applied to a MALDI sample target for analysis. The spectrum was obtained in the positive ion mode utilizing the Reflector mode microchannel plate detector and was generated as the sum of 900−1000 shots.

Ultraviolet-Visible light (UV-Vis) spectroscopy

UV-Vis spectra were recorded on a Cary 5000 UV-Visible IR Spectrophotometer (Agilent Technologies, USA) equipped with a Deuterium UV lamp light source. Spectra were recorded in either THF, *n*-hexane or 50:50 (v/v) THF:*n*-hexane at 20 °C between 200 and 600 nm. Samples were baseline corrected with respect to the pure solvent and measured in a precision cell made of quartz SUPRASIL from HellmaAnalytics.

Dynamic light scattering (DLS)

Dynamic light scattering (DLS) measurements at 90° of the comb polymers in THF, *n*-hexane and 50/50 THF/*n*-hexane (v/v) cosolvent were performed using a DLS detector (Malvern-zetasizer Nano Series) with a 22 mW He–Ne laser operating at 632.8 nm, an avalanche photodiode detector, and an ALV/LSE-5003 multiples digital correlator electronics system. Data analysis of DLS measurements was performed using the CONTIN method.

II. Methods and Procedures

Synthesis of Anthracen-9-ylmethyl bicyclo[2.2.1]hept-5-ene-2-carboxylate (NB-An)

To a 25 mL one neck, round-bottom flask equipped with a magnetic stirrer were charged 5-norbornene-2-carboxylic acid (1.05 g, 1.00 equiv., 7.61 mmol), 4-dimethylaminopyridine (93.0 mg, 0.10 equiv., 0.761 mmol), 9-anthracenemethanol (1.71 g, 1.08 equiv., 8.22 mmol) and CH_2Cl_2 (40 mL). Separately, a solution of *N,N'*-dicyclohexylcarbodiimide (1.73 g, 1.10 equiv., 8.37 mmol) in CH_2Cl_2 was prepared. Both the DCC solution and the main reactor contents were cooled to 0 °C and purged with N_2 for 20 minutes, after which the DCC solution was charged to the reactor via a degassed, gas-tight syringe. The reaction was brought to room temperature and allowed to proceed at room temperature overnight. The crude product was purified via column chromatography with 1:3 *n*-hexane: dichloromethane (R_f = 0.88) to yield a yellow solid (1.77 g, 70.8%). The final product was dried overnight *in vacuo* and characterized via ^{1}H NMR (600 MHz , 25 °C).

^{1}H NMR (600 MHz, $CDCl_3$, 25 °C) δ ppm: 8.50 (s, 1H), 8.32 (d, 2H), 8.01 (d, 2H), 7.61-7.45 (dt, 4H), 6.16 (s, 1H), 6.09 (s, 1H), 5.83 (s, 1H), 3.10 (s, 1H), 2.96 (m, 1H), 2.86 (s, 1H), 1.86 (m, 1H), 1.47 (dt, 1H), 1.34 (m, 1H), 1.20 (d, 1H). ^{13}C NMR (150 MHz, $CDCl_3$, 25 °C) δ 174.95, 137.84, 132.31, 131.41, 131.03, 129.08, 126.65, 126.50, 125.09, 124.05, 58.73, 49.61, 45.84, 43.39, 42.58, 29.25.

Synthesis of oxanorbornene maleimide

The procedure for the synthesis of oxanorbornene maleimide can be found in the work of Yang et al.[2]

Cationic polymerization of polyisobutylene (PIB)

Monofunctional primary bromide-terminated PIB precursor was synthesized by living cationic polymerization of isobutylene followed by *in situ* alkoxybenzene quenching. Polymerization and quenching reactions were performed within a N_2-atmosphere glovebox equipped with a cryostated heptane bath.[2] Synthesis of bromide-terminated PIB was carried out as follows. To a 0.5 L 4-neck round-bottom flask, equipped with an overhead stirrer and ReactIR probe, and immersed in the heptane bath, were added 176 mL anhydrous hexane, 117 mL methyl chloride, 0.14 mL (1.2 mmol, 0.129 g, 0.048 equiv.) 2,6-lutidine, 4.25 mL (25.0 mmol, 3.72 g, 1.00 equiv.) TMPCl initiator, and 98.26 mL (1.19 mol, 66.8 g, 47.6 equiv.) IB. The mixture was equilibrated to -55°C with stirring over 2 h, and polymerization was initiated by the addition of 1.02 mL (9.30 mmol, 1.76 g, 0.22 equiv.) $TiCl_4$. Essentially, full monomer conversion was reached in approximately 4 h according to RT-FTIR data, at which time (3-bromopropoxy)benzene (7.88 mL, 50.0 mmol, 10.8 g, 2.00 equiv.) was charged to the reaction. Additional $TiCl_4$ (10.37 mL, 94.6 mmol, 17.9 g, 3.78 equiv.) was added to catalyze the quenching reaction, resulting in a total $TiCl_4$ concentration of 4.15 eq per chain end. The quenching reaction proceeded for 3 h upon which the catalyst was destroyed by careful addition of excess prechilled methanol (~ 30 mL). The resulting polymer solution was washed with methanol and then precipitated into 0.75 L of methanol and acetone solution (methanol/acetone, v/v, 95/5). The precipitate was collected by re-dissolution in fresh hexane; the solution was washed with

DI water and dried over $NaSO_4$. Residual solvent was removed under vacuum at 50 °C to yield pure primary bromide-terminated PIB precursor (M_n = 3.34 kg/mol, $Đ$ =1.19.)

^{1}H NMR ($CDCl_3$, 600 MHz): δ = 6.82 (ml, 2-H), 4.09 (t, 2-H), 3.61 (t, 2H), 2.31 (m, 2-H), 1.80 (s, l2-H), 1.43 (br, 99-H), 1.12 (br, 299l-H).

Synthesis of oxanorbornene maleimide polyisobutylene (oNBMIPIB)

Monofunctional primary bromide-terminated PIB precursor (6 g, M_n=3.35 kg/mol, PDI=1.19) was dissolved in 200 mL of freshly distilled THF, and the solution was transferred to a 500 mL one-neck round bottom flask. To the stirred solution were added 40 mL of anhydrous N-methyl-2-pyrrolidone (NMP), 0.910 g (5.52 mmol, 2.98 equiv.) exo-7-oxanorbornene-2,3-dicarboximide, 1.27 g (9.2 mmol, 1.66 equiv.) potassium carbonate, and 0.97 g (15.3 mmol, 2.49 equiv.) 18-crown-6. The mixture was heated at 50 °C under a dry N_2 atmosphere for 14 h. Upon completion of the reaction, the THF was vacuum stripped, and the polymer was dissolved in *n*-hexane. The resulting solution was filtered through a filter paper and slowly added into excess methanol to precipitate the polymer. The precipitate was re-dissolved in fresh hexane, and the resulting solution was washed with DI water, dried over $NaSO_4$, and then vacuum stripped at room temperature to obtain pure oNBMIPIB (M_n = 3.5 kg/mol, $Đ$ = 1.21).

^{1}H NMR (CDCl3, 600 MHz): δ = 6.79 (t, 2-H), 6.50 (s, 2-H), 5.25 (s, 2-H), 3.94 (t, 2-H), 3.70 (t, 2H), 2.85 (s, 2-H), 2.08 (m, 2-H), 1.821 (s, 2-H), 1.43 (br, 100-H), 1.12 (br, 300-H).

In situ ^{1}H NMR kinetic study of ring-opening metathesis polymerization (ROMP) of NB-An

An NMR tube with a pierceable rubber septum was charged with a solution of NB-An (20.5 mg, 0.187 mmol, 500 equiv.) in dry CD_2Cl_2 (0.5 mL). The tube was submerged in an ice bath, and the solution was sparged with N_2 for 10 min. The NMR tube was warmed to room temperature and an initial ^{1}H NMR (600 MHz, 25 °C) spectrum was acquired. Separately, a stock solution of G3 ([G3] = 0.0115 M) was prepared in a glovebox by adding G3 (8.55 mg, 0.0115 mmol) and dry DCM (1 mL) to an oven dried 8 mL vial with a pierceable cap. Polymerization was initiated by charging to the NMR tube a stock solution of G3 catalyst (21.66 µL) via a degassed, gas-tight syringe, such that the initial conditions of $[NB\text{-}An]_0$ = 0.125 M and $[G3]_0$ = 0.25 mM were achieved ($DP_{n,\ target}$ = 500). A scan was acquired every 30 s for 15 min to monitor the polymerization. Conversion was determined by taking the relative integration of the 10-anthracene proton peak of the monomer at 8.57 ppm (1H) compared to the total combined aromatic proton peaks of monomer and polymer from 7.15 to 8.63 ppm (9H).

Ring-opening metathesis polymerization (ROMP) of NB-An

An oven-dried scintillation vial with a pierceable cap was charged with a stir bar and a solution of NB-An (131.3 mg, 0.4 mmol, 200 equiv.) in dry CH_2Cl_2 (8 mL). The vial was submerged in an ice bath, and the solution was sparged with N_2 for 10 min. Separately, a stock solution of G3 ([G3] = 0.013 M) was prepared in a glovebox by adding G3 (9.65 mg, 0.013 mmol) and dry DCM (1 mL) to an oven dried 8 mL vial with a pierceable cap. The vial was warmed to room temperature, and with vigorous stirring, polymerization was initiated by charging to the vial a stock solution of G3 catalyst via a degassed, gas-tight syringe, such that the initial conditions of $[G3]_0$= 0.25 mM and $[NB\text{-}An]_0$ = 0.05 M were achieved. After 8 min, the reaction was quenched with an excess of ethyl vinyl ether (~ 0.2 mL) and allowed to stir for 30 additional minutes. The catalyst was removed by passing the reaction solution through a short silica plug. The filtered solution

was concentrated under reduced pressure and precipitated twice into MeOH. The final polymer was dried *in vacuo* overnight and characterized by ^{1}H NMR (600 MHz, 25 ^{o}C) and GPC.

^{1}H NMR (600 MHz, CDCl3) δ 8.21(br, 3H), 7.79(br, 2H), 7.32(br, 4H), 5.98(br, 2H), 5.09(br, 2H), 2.67(br, 3H), 1.70(br, 2H), 1.27(br, 2H).

Ring-opening metathesis copolymerization (ROMP) of NB-An and oNBMIPIB, with slow addition of NB-An (P1 and P2).

An oven-dried 4 mL vial with a pierceable cap was charged with a stir bar and oxanorbornene maleimide polyisobutylene (oNBMIPIB) (P1: 151.2 mg, 0.043 mmol, 120 equiv.; P2: 131.9 mg, 0.038 mmol, 90 equiv.) in dry CH_2Cl_2 (1.2 mL). Separately, a solution of NB-An (P1: 3.49 mg, 0.010 mmol, 30 equiv.; P2: 7.47 mg, 0.022 mmol, 60 equiv.) was prepared in a vial with dry CH_2Cl_2 (0.3 mL). Both solutions were sparged with N_2 on ice for 30 minutes. Separately, a stock solution of G3 ([G3] = 0.013 M) was prepared in a glovebox by adding G3 (9.65 mg, 0.013 mmol) and dry DCM (1 mL) to an oven dried 8 mL vial with a pierceable cap. The NBAn solution was drawn into a degassed, gas-tight syringe and placed into a preset syringe pump. The polymerization was initiated by adding the stock solution of G3 (28.79 µL) to the vigorously stirring reaction vessel such that the initial conditions of $[oNBMIPIB]_0$ = 0.03 M or 0.0225 M for P1 and P2, respectively, and $[G3]_0$= 0.25 mM were achieved. Simultaneously, the syringe pump was turned on to deliver a constant feed (P1: 0.30 mL/hr; P2: 0.44mL/hr) of NBAn for the reaction duration such that $[NB\text{-}An]_o$ = 0.0075 M or 0.015 M for P1 and P2, respectively. After 60 or 45 minutes, the reaction was quenched with an excess of ethyl vinyl ether (~ 0.2 mL) and allowed to stir for 30 additional minutes. The catalyst was removed by passing the reaction solution through a short silica plug. The filtered solution was concentrated under reduced pressure and precipitated twice into MeOH. The final polymer was dried *in vacuo* overnight and characterized by ^{1}H NMR (600 MHz, 25 ^{o}C) and GPC.

^{1}H NMR (600 MHz, $CDCl_3$, 25 ^{o}C) δ ppm: 8.26 (br, 3H, Ph-*H*), 7.84(br, 2H, Ph-*H*), 7.39(br, 4H, Ph-*H*), 6.75(s, 2H, Ph-*H*), 5.81(br, 2H), 5.07(br, 2H), 4.46(br, 2H), 3.92(br, 2H), 3.68(br, 2H), 3.31(br, 2H), 2.04(br, 2H), 1.62-0.60(br, XH).

Ultraviolet-Visible light (UV-Vis) spectroscopy kinetic experiment.

Two separate means were used to prepare samples for UV-Vis absorption spectroscopy,

1. A stock solution (c = 6.4 mg·mL^{-1}) was prepared by dissolving 12.8 mg of P1 in 2 mL of THF via micropipette. The solution was diluted to a concentration of 1 mg/mL by the addition of 0.625 mL of stock solution to 3.375 mL of THF performed via micropipette (Fisherbrand 100-1000 µL). The solution was further diluted to 0.5 mg/mL in a cosolvent of THF/*n*-hexane via the addition of 1 mL of the 1 mg·mL^{-1} solution in THF to a separate vial and the subsequent addition of 1 mL of *n*-hexane via micropipette (Fisherbrand 100-1000 µL).
2. A stock solution (c = 1.004 mg·mL^{-1}) was prepared by dissolving 5.02 mg of P2 in approximately 3 mL of THF. The solution was then transferred to a 5 mL volumetric flask and filled until the endpoint was reached. The solution was further diluted down (c = 0.5 mg·mL^{-1}) via the addition of one mL of the 1.004 mg·mL^{-1} via gas-tight syringe and 1 mL of *n*-hexane via gas-tight syringe. The solution was allowed five minutes of equilibration before irradiation.

III. Characterization of PIB functionalization and polymerization

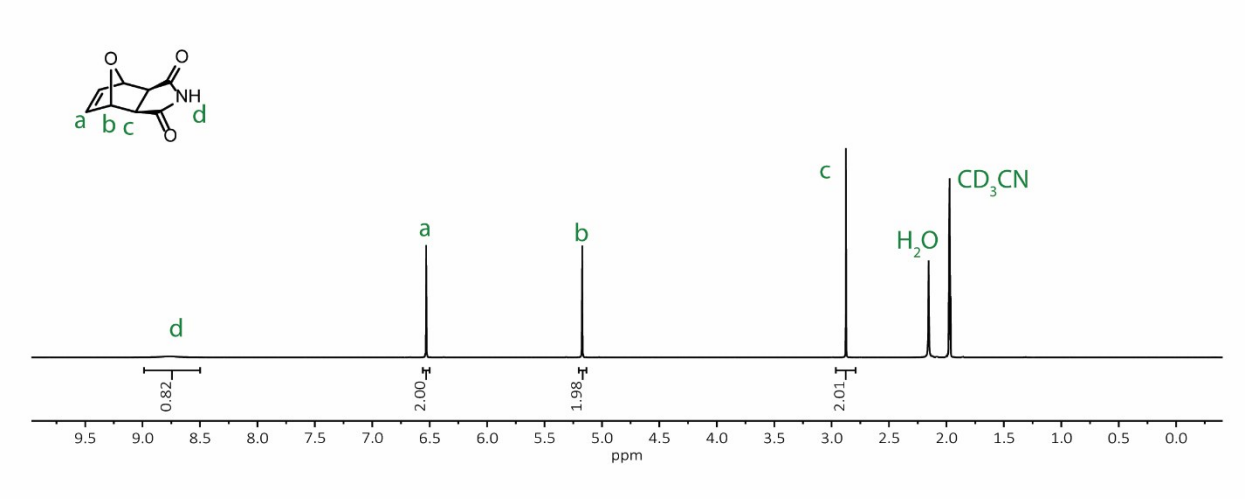

Figure S1. ^{1}H NMR spectrum of exo-7-oxanorbornene-2,3-dicarboximide in CD_3CN.

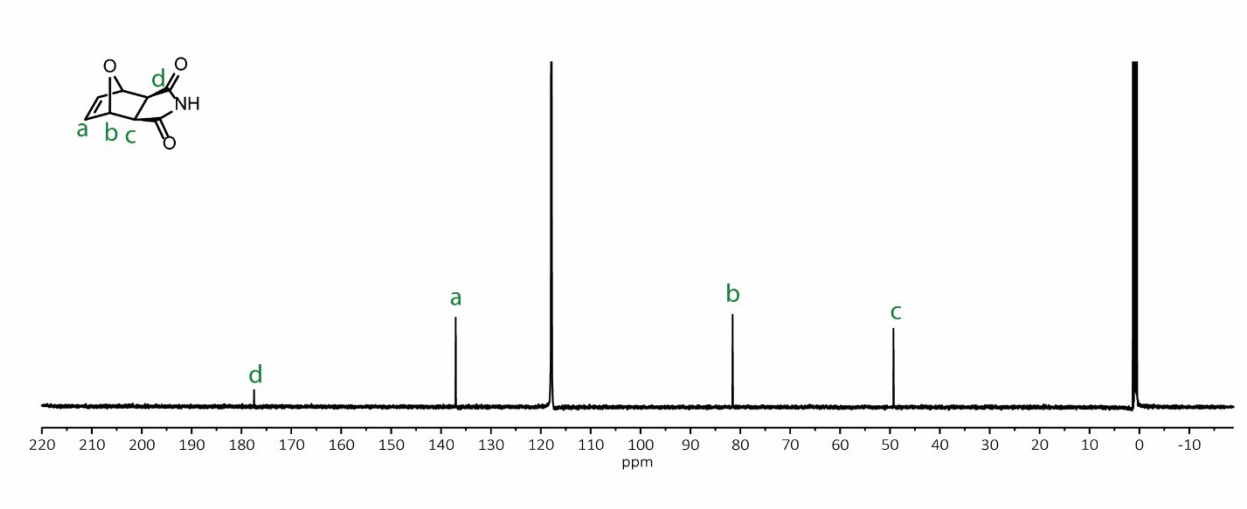

Figure S2. ^{13}C NMR spectrum of exo-7-oxanorbornene-2,3-dicarboximide in CD_3CN.

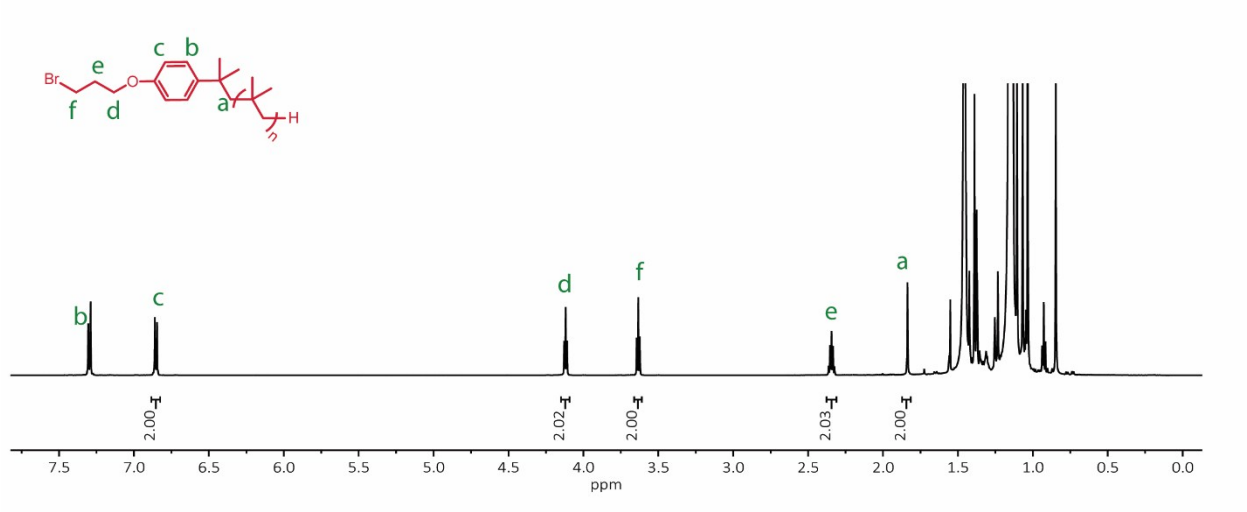

Figure S3. ^{1}H NMR spectrum of PIB-Br in $CDCl_3$.

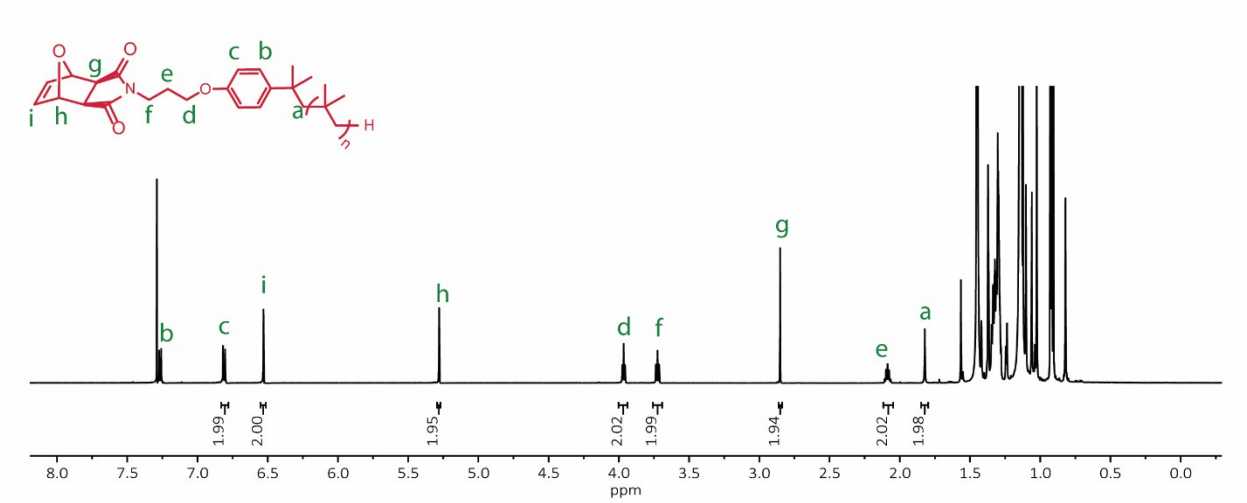

Figure S4. ^{1}H NMR spectrum of oxanorbornene maleimide polyisobutylene (oNBMIPIB) in $CDCl_3$.

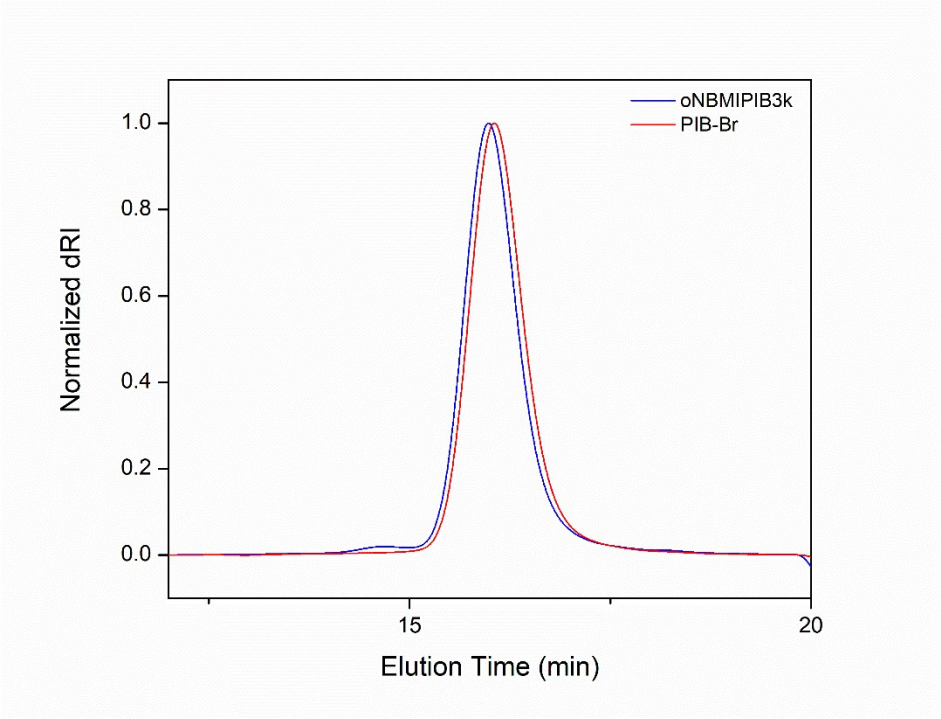

Figure S5. SEC elugrams of PIB-Br (red) and oxanorbornene maleimide polyisobutylene (oNBMIPIB) (blue).

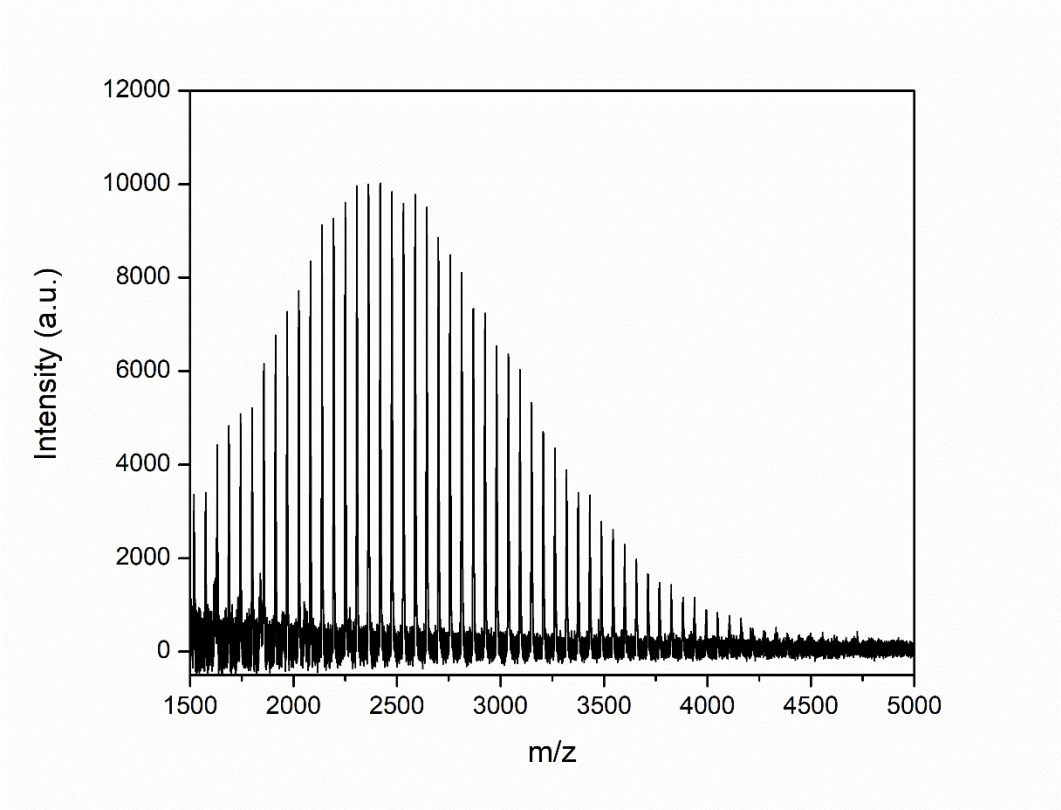

Figure S6. MALDI-TOF mass spectrum of oxanorbornene maleimide polyisobutylene (oNBMIPIB). The spectrum shows only one distribution of homologues, indicating high fidelity to the theoretical structure and exclusively Ag cations from the AgTFA cationizing agent.

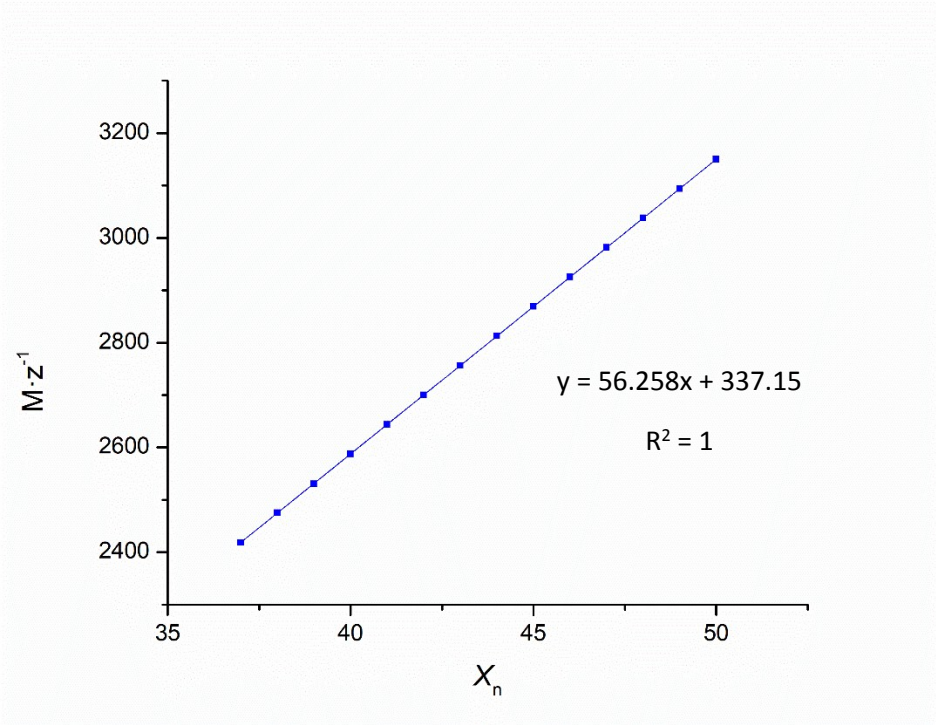

Figure S7. Plot of m/z vs. degree of polymerization of the single distribution of homologues observed in the MALDI-TOF mass spectrum of oxanorbornene maleimide polyisobutylene. Linear regression indicated a repeat unit mass of 56.248 Da and a residual mass of 337.15 Da. Based on the expected structure, the residual mass should be equal to $C_{17}H_{17}O_4N^{107}Ag$ (406.02 Da). The difference of 68.87 Da is very close to the mass of furan (68.03 Da), indicating that the chain ends underwent a retro Diels Alder reaction due to the high vacuum and temperature utilized in MALDI-TOF mass spectroscopy. This phenomenon was anticipated, having been previously reported by Wang et al.[2]

IV. Characterization of NB-An monomer and polymer

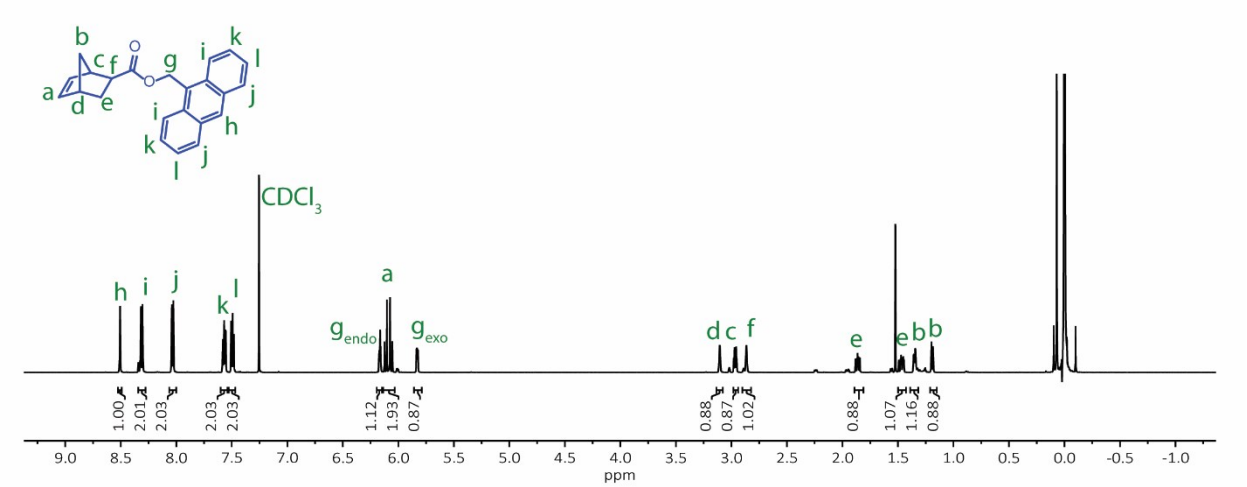

Figure S8. ^{1}H NMR spectrum (600 MHz, 25 ^{o}C) of anthracen-9-ylmethyl bicyclo[2.2.1]hept-5-ene-2-carboxylate (NB-An) in $CDCl_3$.

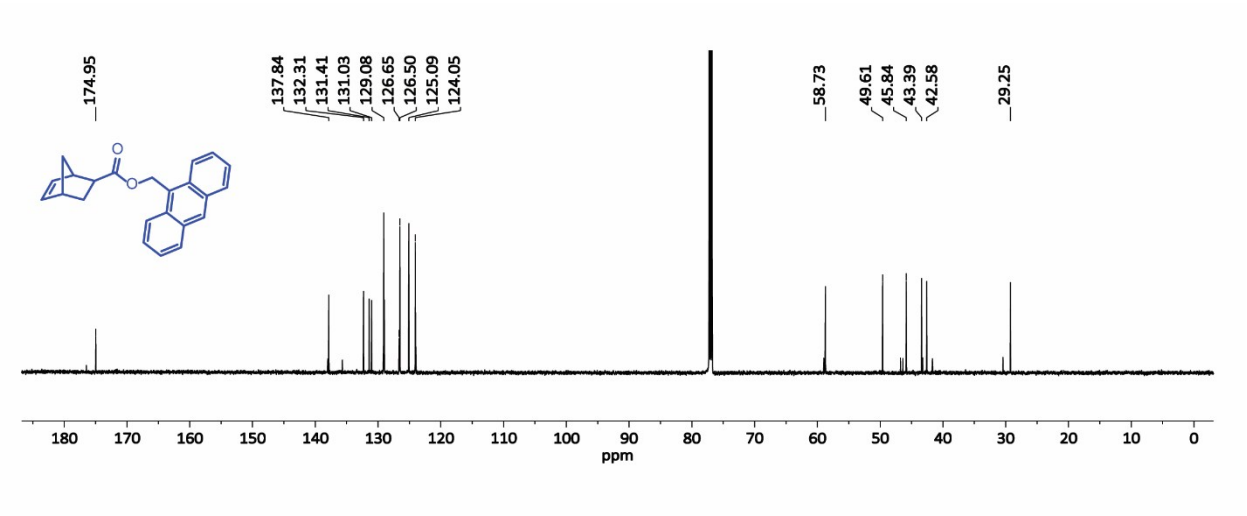

Figure S9. ^{13}C NMR (150 MHz, 25 ^{o}C) of anthracen-9-ylmethyl bicyclo[2.2.1]hept-5-ene-2-carboxylate (NB-An) in $CDCl_3$.

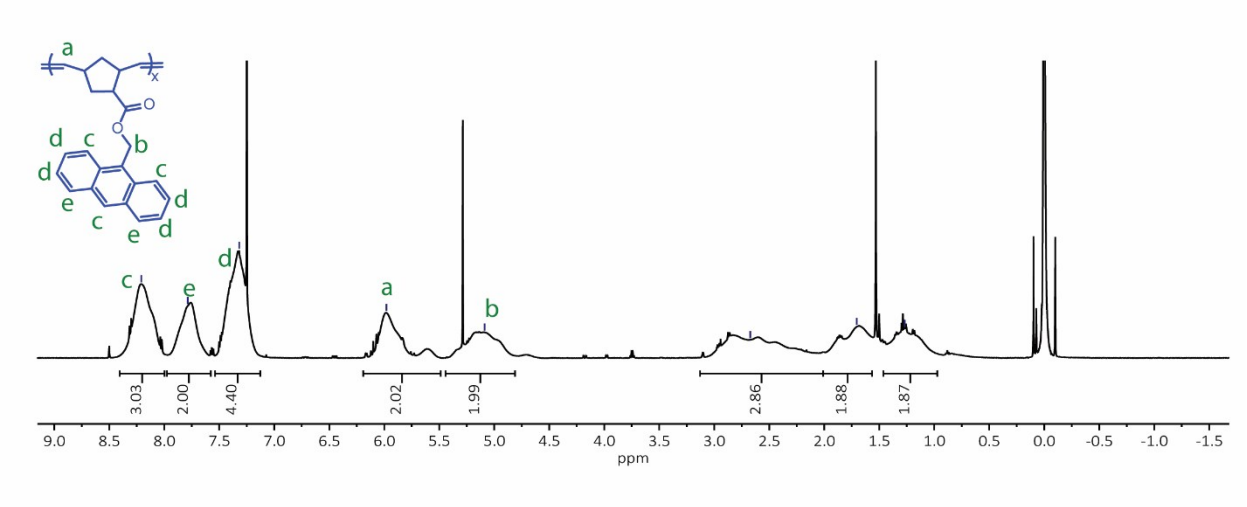

Figure S10. ^{1}H NMR spectrum (600 MHz, 25 ^{o}C) of PNB-An in $CDCl_3$.

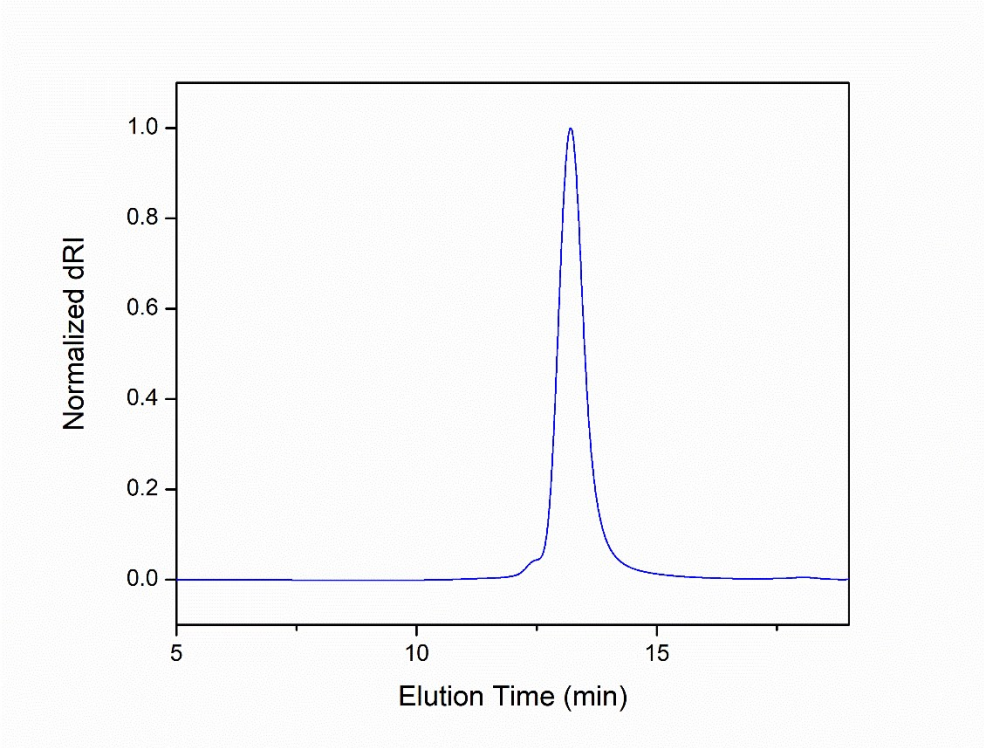

Figure S11. SEC elugram of PNB-An, DP_n = 200 (M_n = 70.3 kg/mol, M_w = 75.0kg/mol, $Đ$ = 1.06).

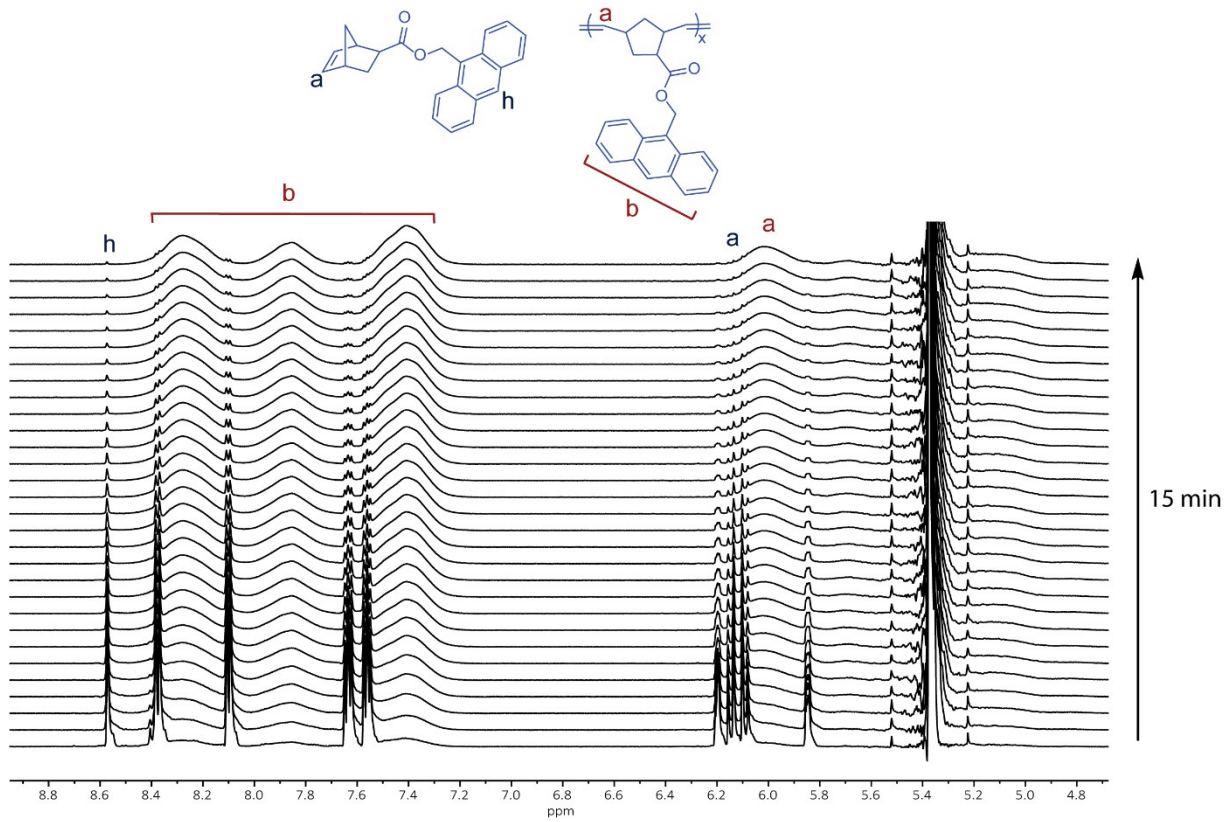

Figure S12. Representative *in situ* ^{1}H NMR (600 MHz, 25 °C) stack of ROMP of NB-An at 23 °C in CD_2Cl_2. Each spectrum corresponds to a 30 second delay interval over the course of 15 minutes. The disappearance of the anthracenyl monomer peak at 8.57 ppm relative to the overall monomeric and polymeric anthracenyl integration from 7.15 to 8.63 ppm was used to monitor conversion over time.

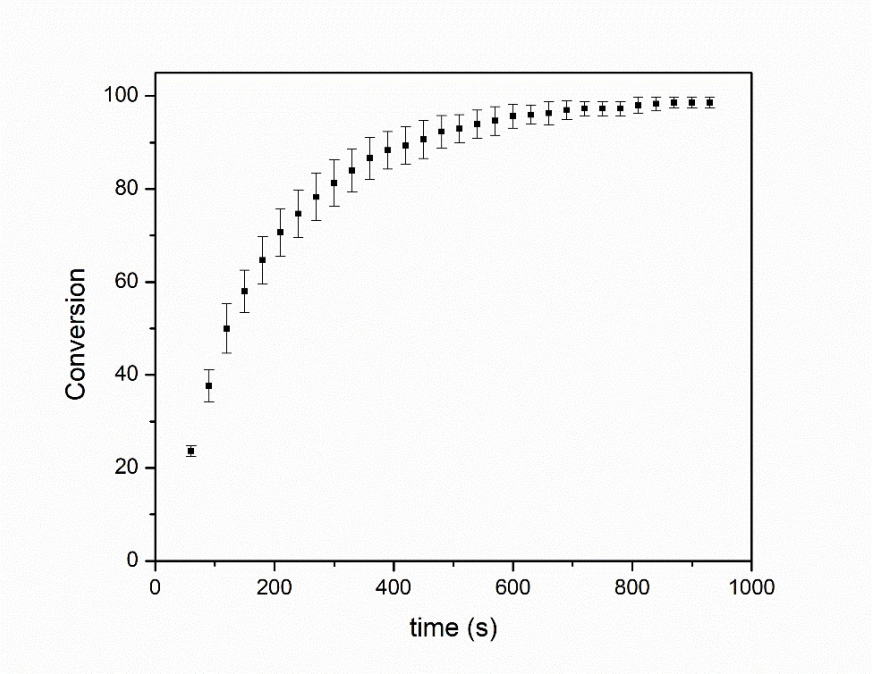

Figure S13. Conversion versus time plot of ROMP of NB-An at 23 °C, generated from *in situ* ^{1}H NMR (600 MHz, 25 ^{o}C) data. Samples were run in triplicate.

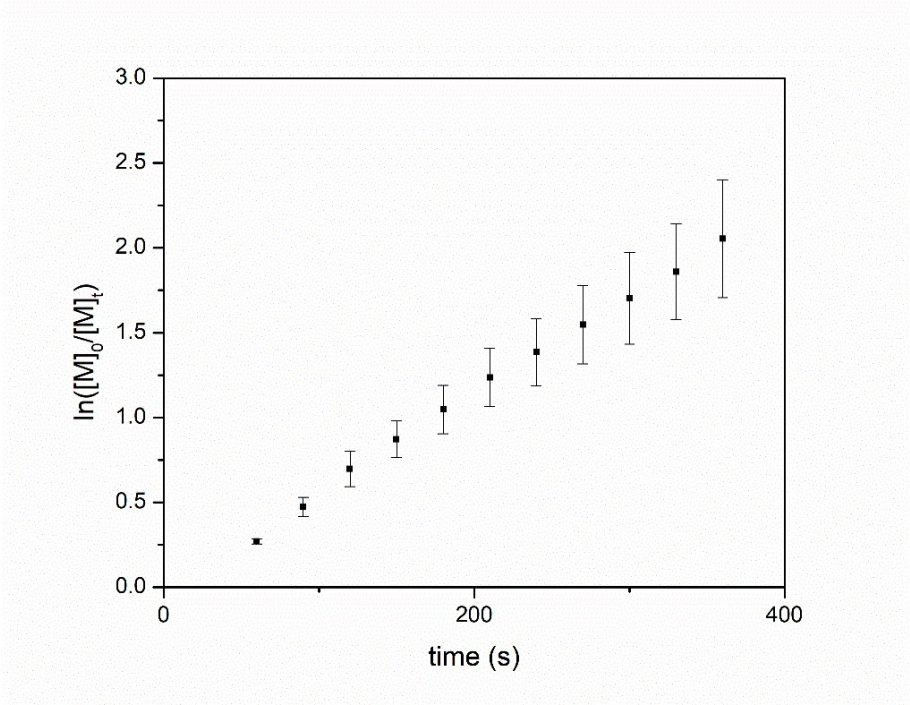

Figure S14. Semilogarithmic kinetic plot of *in situ* ^{1}H NMR (600 MHz, 25 ^{o}C) kinetic study of ROMP of NB-An. Points were taken from the linear regime of the conversion versus time plot. Samples were run in triplicate.

Table S1. Summary of kinetic ROMP of PNB-An

Homopolymer	[M]:[G3]	$[G3]_0$ (mM)	k_{obs} (10^{-3} s^{-1})[b]	R^2	$t_{1/2}$ (s)[c]	k_{homo} (10^{-3} M^{-1} s^{-1})[d]
PNB-An	500	0.25	5.81	0.997	119	23.24
PoNBMIPIB[a]	100	0.27	2.33	-	297	4.93

[a] Value reported by Yang et al.[2]

[b] Slope of the semilogarithmic plot from Figure S14.

[c] Calculated using $t_{1/2} = \ln(2)/k_{obs}$.

[d] k_{homo}, which is independent of catalyst concentration, was calculated using $k_{homo} = k_{obs}/[G3]_0^3$

In general, it is understood that macromonomers polymerize via ROMP at a slower rate than small molecule monomers, largely due to inherent steric congestion prevalent in macromonomers. For comonomers with great disparity in homopolymerization rate constants, k_{homo}, it is highly unlikely that a batch copolymerization via ROMP would result in a statistically random copolymer. Thus, for this work it was imperative to determine the k_{homo} for each monomer to understand the relative difference in polymerization rate, and if necessary, to switch from a batch copolymerization to a semi-continuous copolymerization in which the more reactive monomer is added dropwise over the course of the copolymerization. For PoNBMIPIB, the value for k_{obs} was reported by Yang et al.[2] to be $2.33 \cdot 10^{-3}$ s^{-1}. It is important to note that $[G3]_0$ and target DP_n in those experiments were different than the equivalent $[G3]_0$ and target DP_n used in this study. To account for this, k_{homo}, a rate constant that is independent of the catalyst concentration used, can be calculated by the equation $k_{homo} = k_{obs}/[G3]_0^3$. In doing so, it was found that $k_{homo,\ PNB\text{-}An}$ was approximately 2.6 times greater than $k_{homo,\ PoNBMIPIB}$. As a result, the copolymerizations for P1 and P2 in our study utilized the slow-addition copolymerization method to ensure NB-An was evenly distributed throughout the comb copolymer backbone.

V. Characterization of PNB-An-co-PoNBMIPIB copolymers

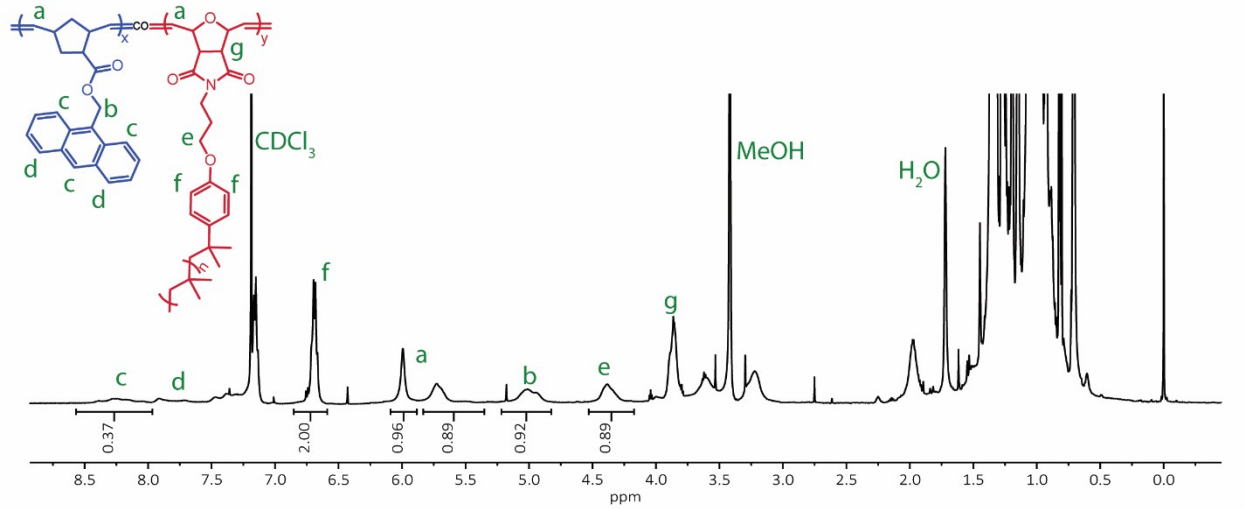

Figure S15. ^{1}H NMR spectrum (600 MHz, 25 ^{o}C) of poly(norbornene anthracene)-*co*-poly(oxanorbornene maleimide polyisobutylene) (PNBAn-co-PoNBMIPIB) P1 in $CDCl_3$.

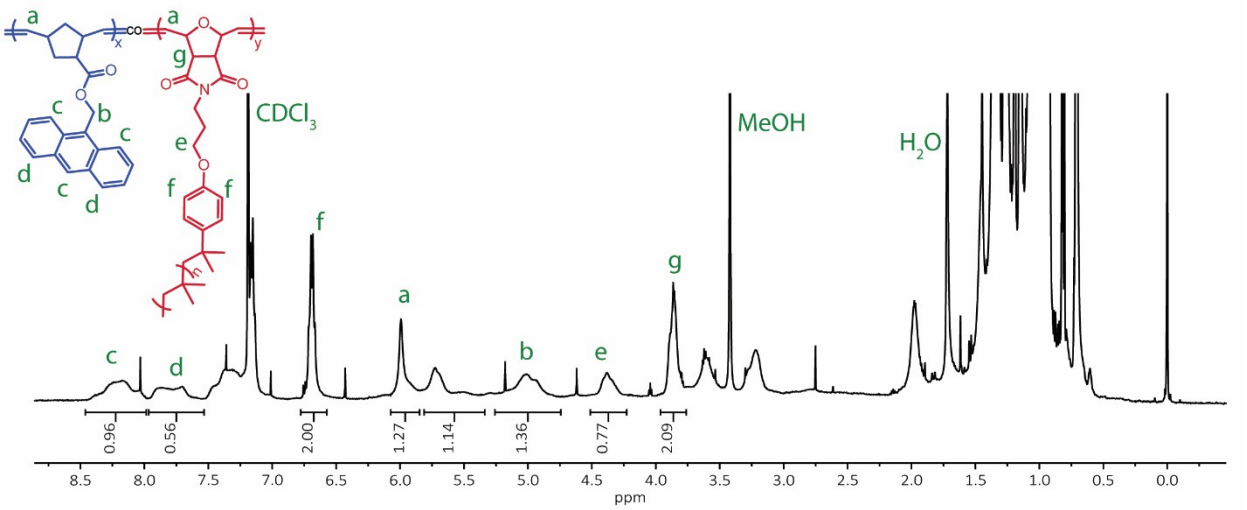

Figure S16. ^{1}H NMR spectrum (600 MHz, 25 ^{o}C) of poly(norbornene anthracene)-*co*-poly(oxanorbornene maleimide polyisobutylene) (PNBAn-co-PoNBMIPIB) P2 in $CDCl_3$.

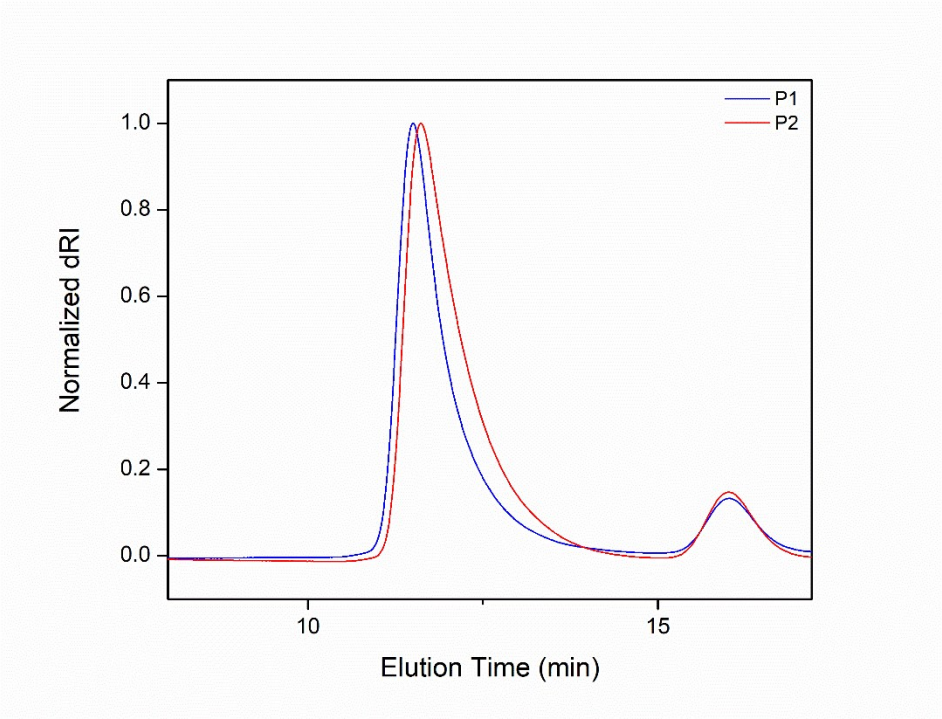

Figure S17. SEC (refractive index detector) of poly(norbornene anthracene)-*co*-poly(oxanorbornene maleimide polyisobutylene) (PNBAn-co-PoNBMIPIB) P1 (blue) and P2 (red).

VI. UV-Vis data correction

During data collection, a regular baseline error was observed due to a switchover from a near-infrared to a UV light source in which the baseline artificially jumped to a higher absorbance. This higher absorbance was found to noticeably affect subsequent measurements. To correct for this inaccuracy, the switchover point was manually located and corrected where the difference in absorbance directly before and after the switchover point was added back into the baseline of subsequent UV-Vis spectra. This corrective process was done for Figure 2d in the main document. The general corrective process is shown in Figures S18 through S20 below.

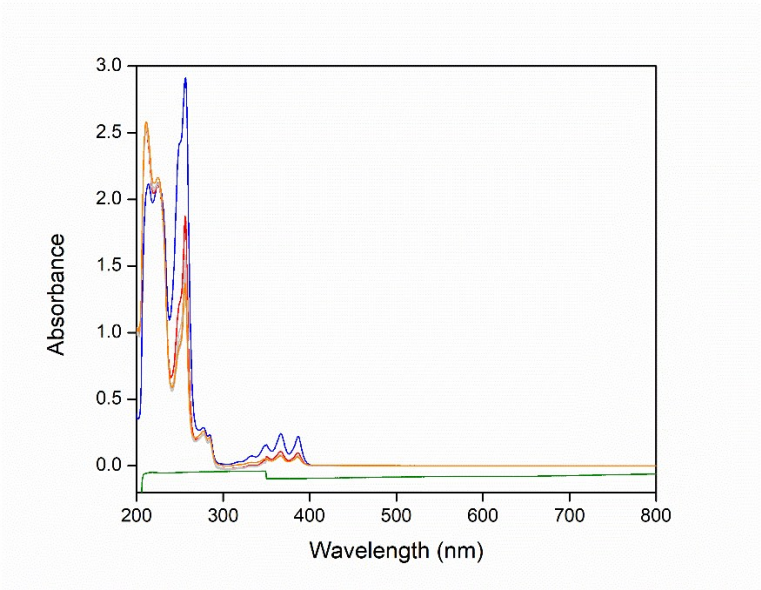

Figure S18. Full spectra for the raw data of P1 included in Figure 2d. The absorbance from λ = 200 to 300 nm corresponds to the aliphatic region of the copolymer P1. The instrument baseline (green) observed an increase in absorbance by 0.0299 at λ = 350 nm.

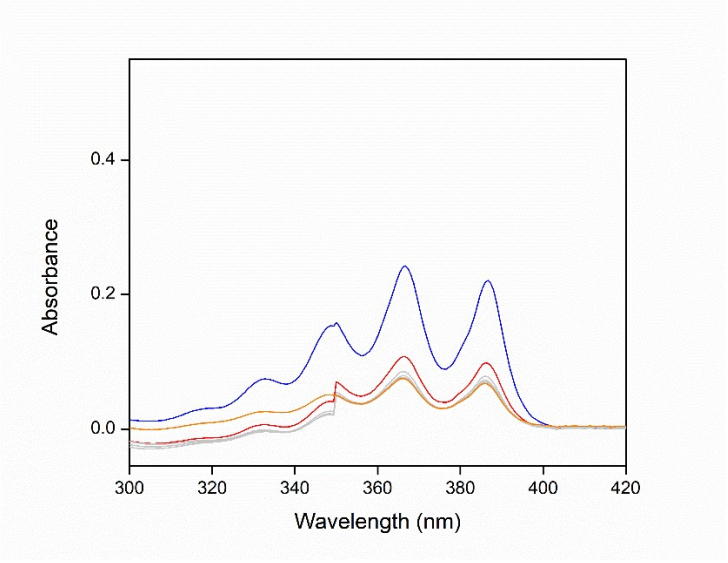

Figure S19. Uncorrected spectra for Figure 2d with baseline error (baseline is not pictured here).

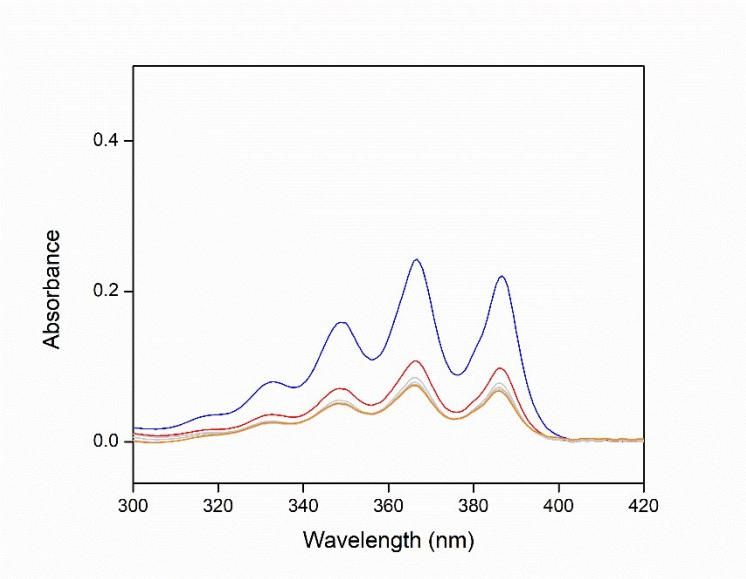

Figure S20. Corrected spectra for Figure 2d when accounting for the baseline error.

VII. Irradiation studies and characterization of P1 and P2

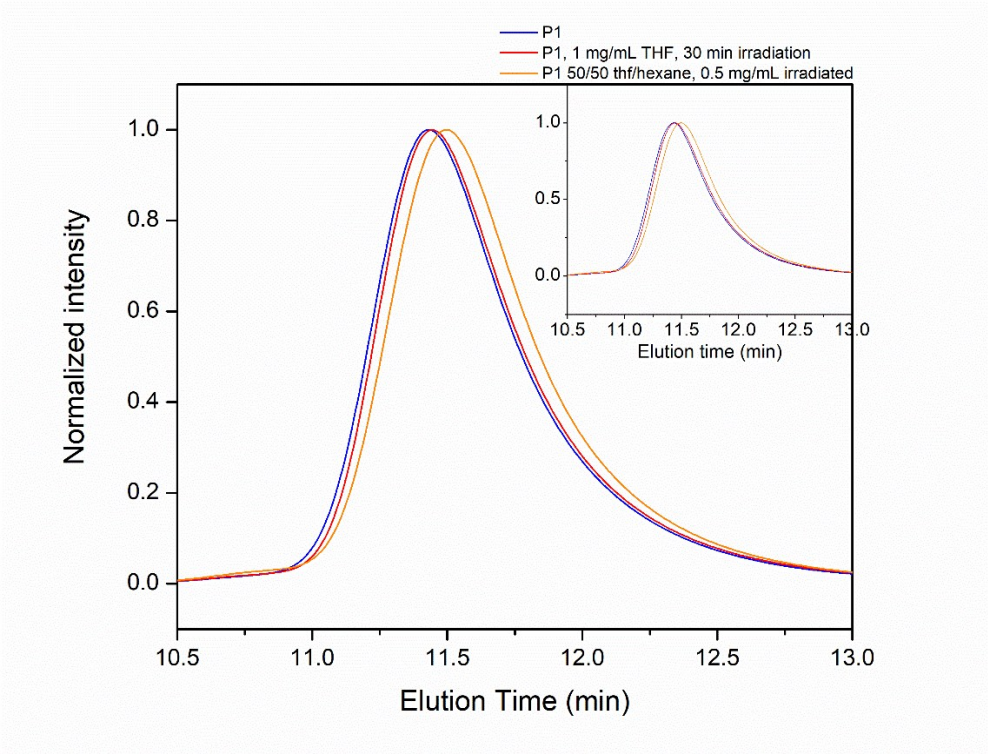

Figure S21. SEC (MALS detector) of P1 in THF (blue), irradiated in THF (c = 1 mg·mL^{-1}, red), and sequential irradiation in 50/50 THF/*n*-hexane (v/v) (c = 0.5 mg·mL^{-1}, orange) (Inset: dRI detector).

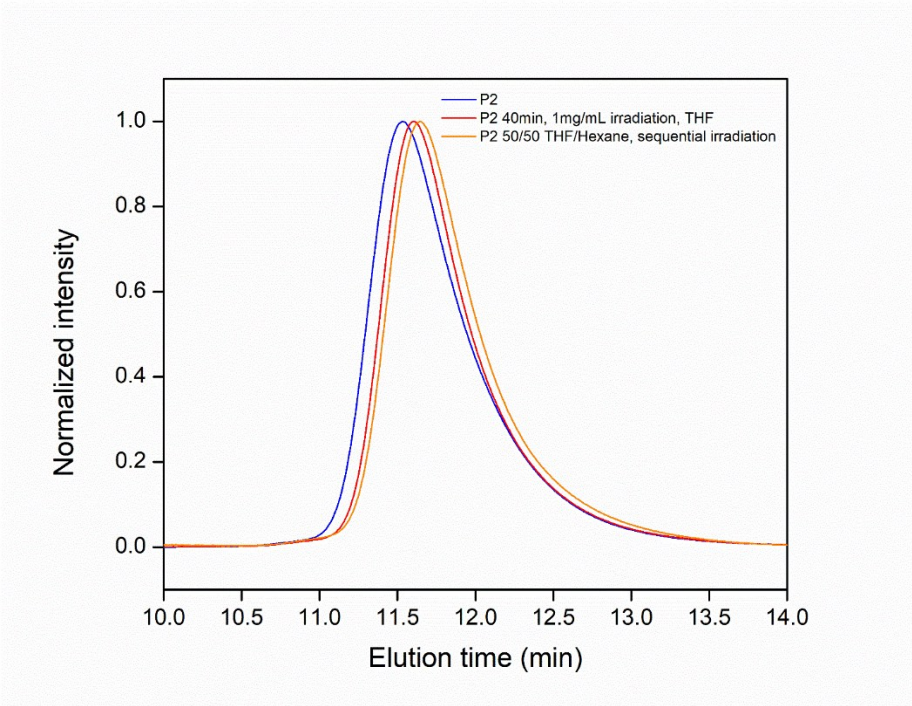

Figure S22. SEC (MALS detector) of P2 in THF (blue), irradiated in THF (c = 1 mg·mL^{-1}, red), and sequential irradiation in 50/50 THF/*n*-hexane (v/v) (c = 0.5 mg·mL^{-1}, orange).

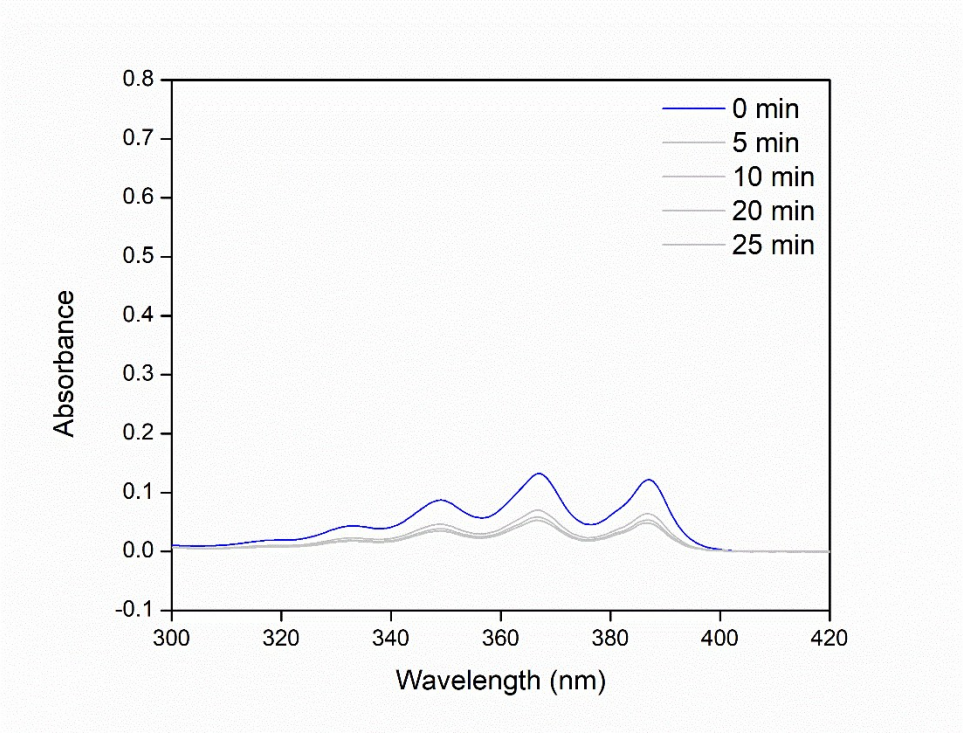

Figure S23. UV-Vis spectra of P1 (blue) and irradiated P1 (grey) in THF (c = 0.5 mg·mL^{-1})

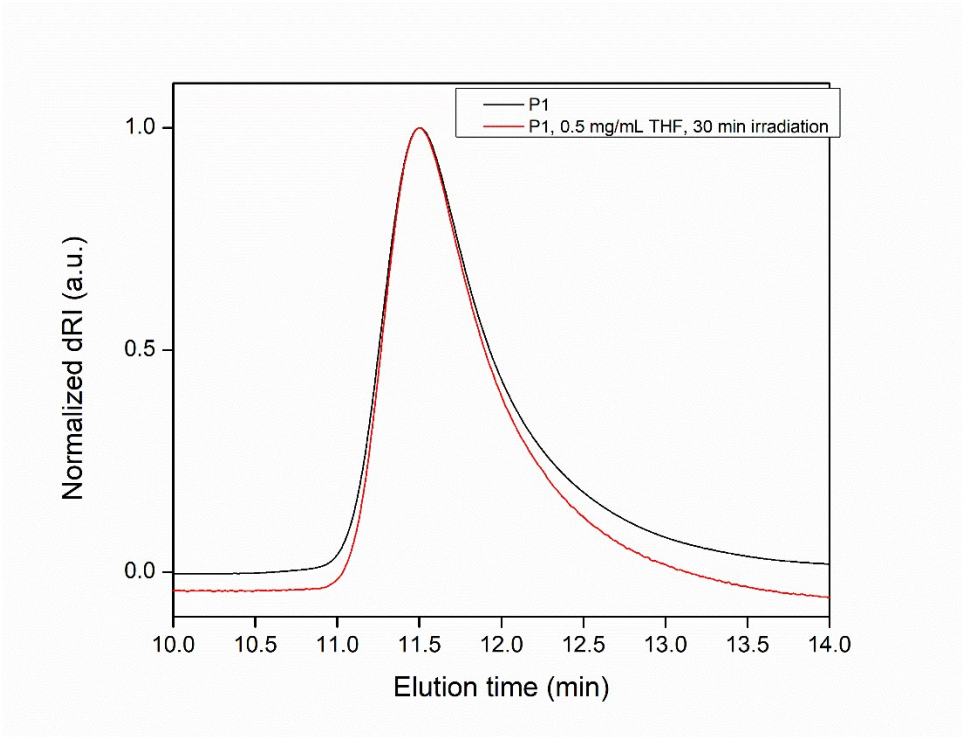

Figure S24. SEC elugram (refractive index detector) of pristine P1 (black) and irradiated P1 (red) in THF (c = 0.5 mg·mL^{-1})

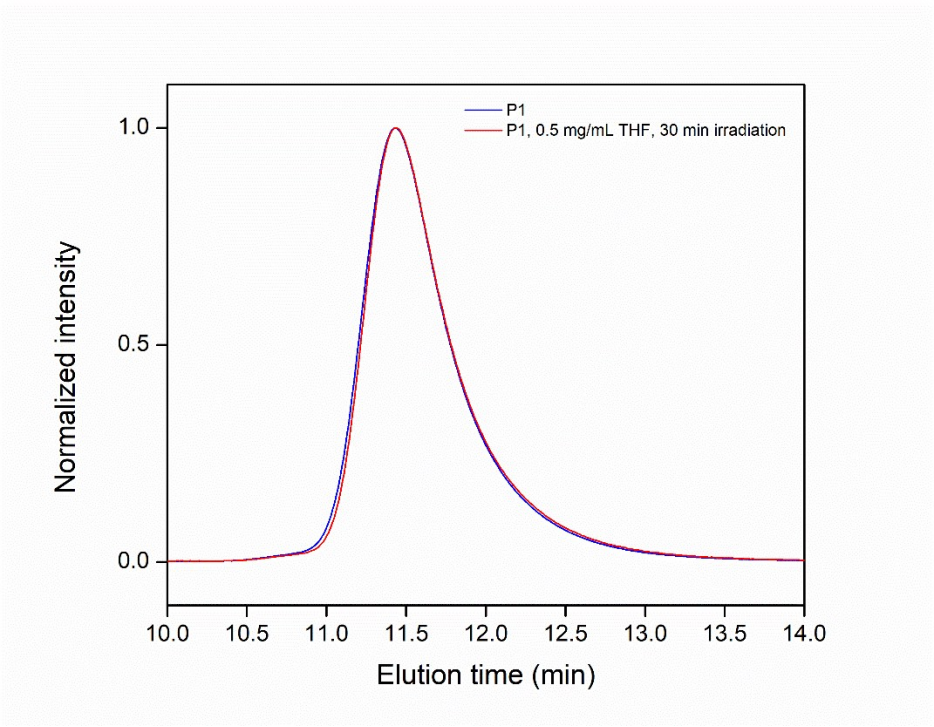

Figure S25. SEC elugram (MALS detector) of pristine P1 (blue) and irradiated P1 (red) in THF (c = 0.5 mg·mL^{-1})

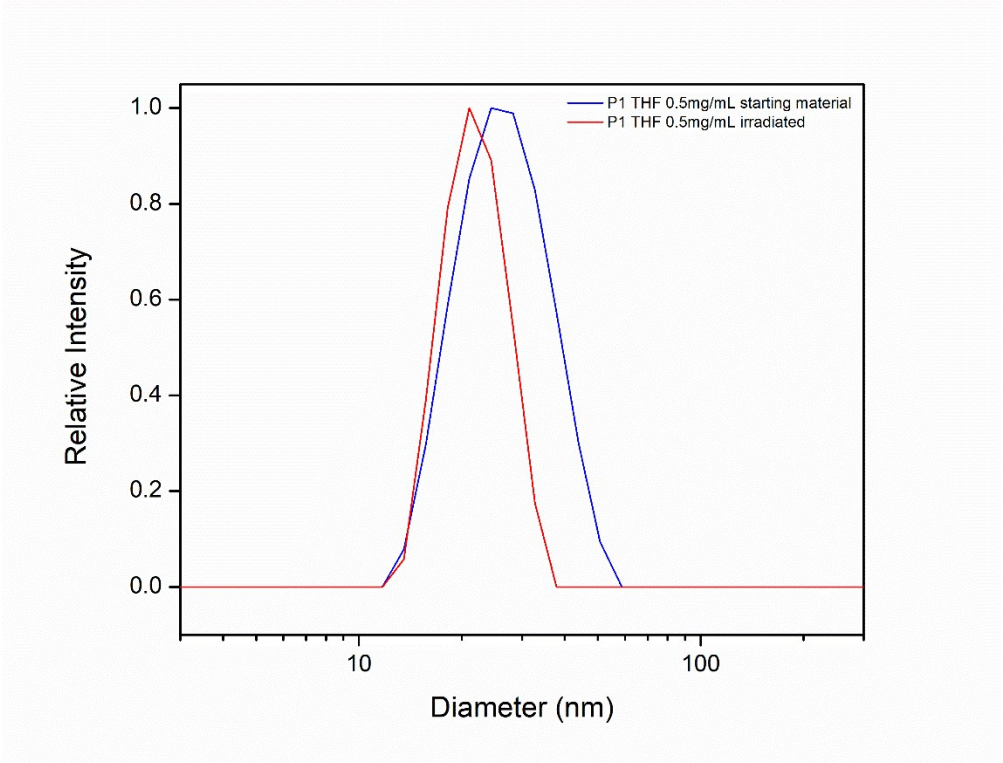

Figure S26. DLS distribution of pristine P1 (blue) and irradiated P1 (red) in THF (*c* = 0.5 mg·mL^{-1})

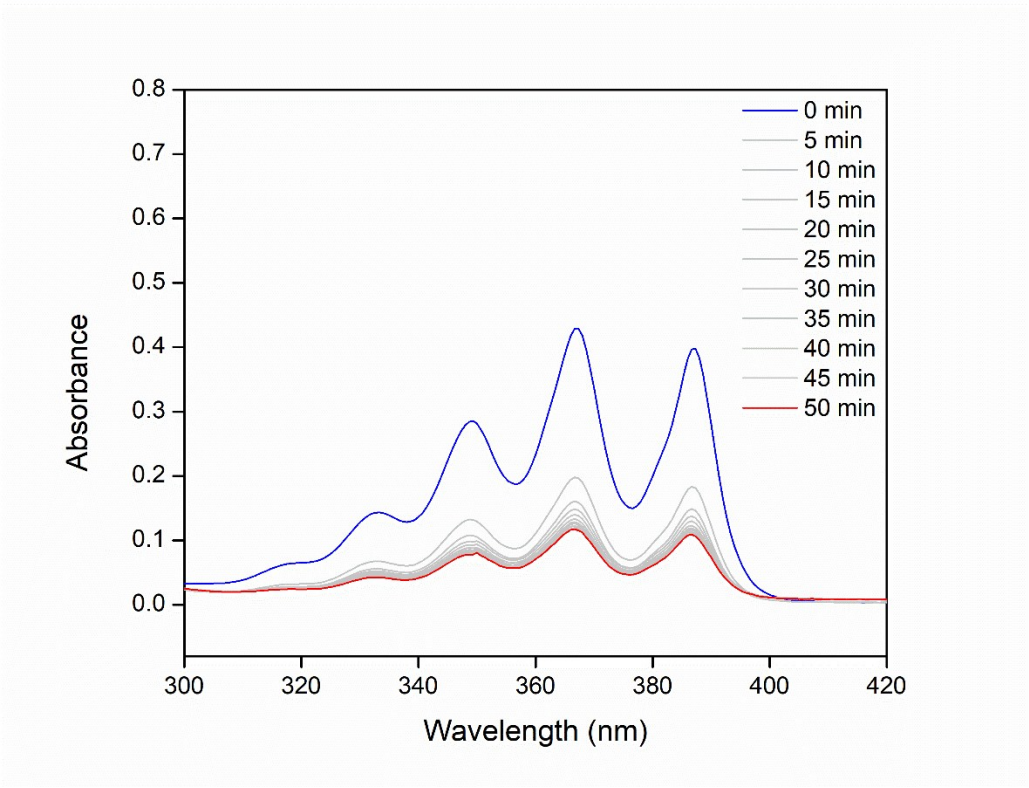

Figure S27. UV-Vis spectra of P2 (blue) and irradiated P2 (red) in THF (*c* = 0.5 mg·mL^{-1})

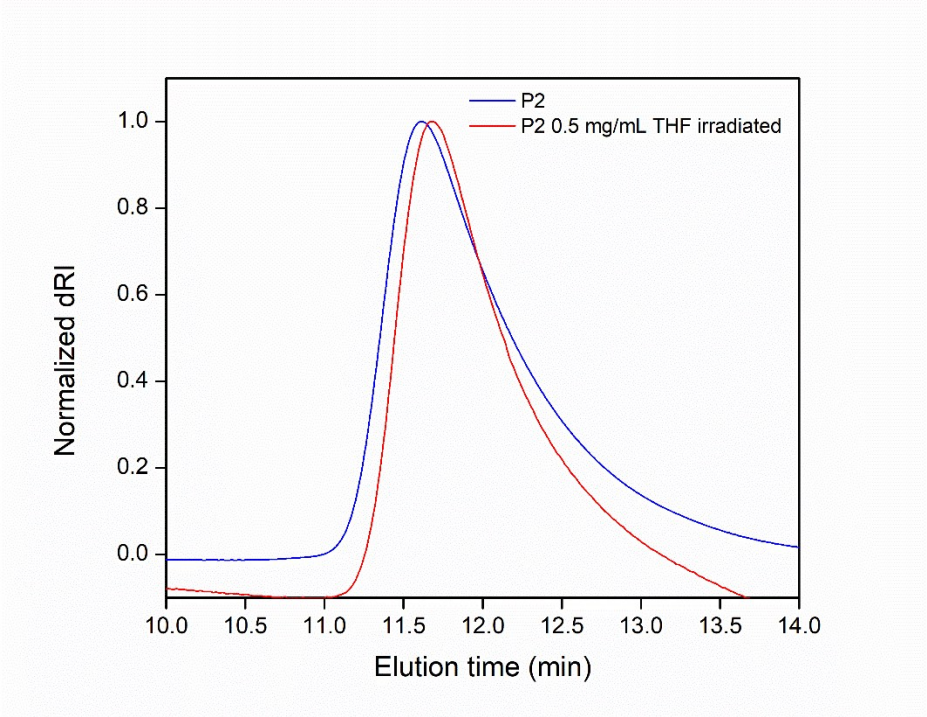

Figure S28. SEC elugram (dRI detector) of pristine P2 (blue) and irradiated P2 (red) in THF (c = 0.5 mg·mL^{-1})

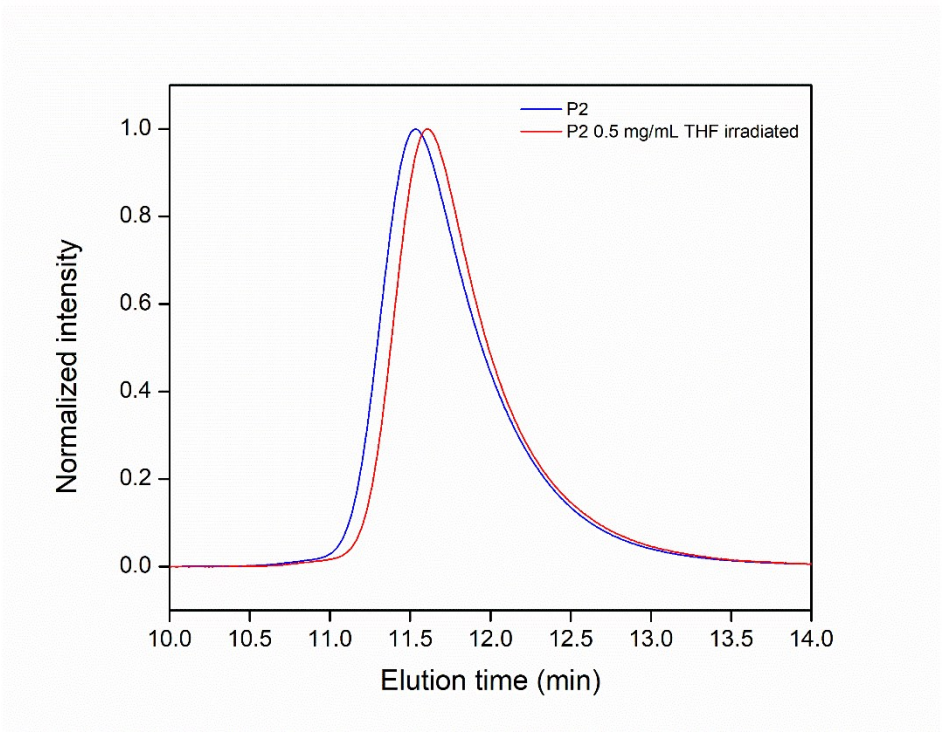

Figure S29. SEC elugram (MALS detector) of pristine P2 (blue) and irradiated P2 (red) in THF (c = 0.5 mg·mL^{-1})

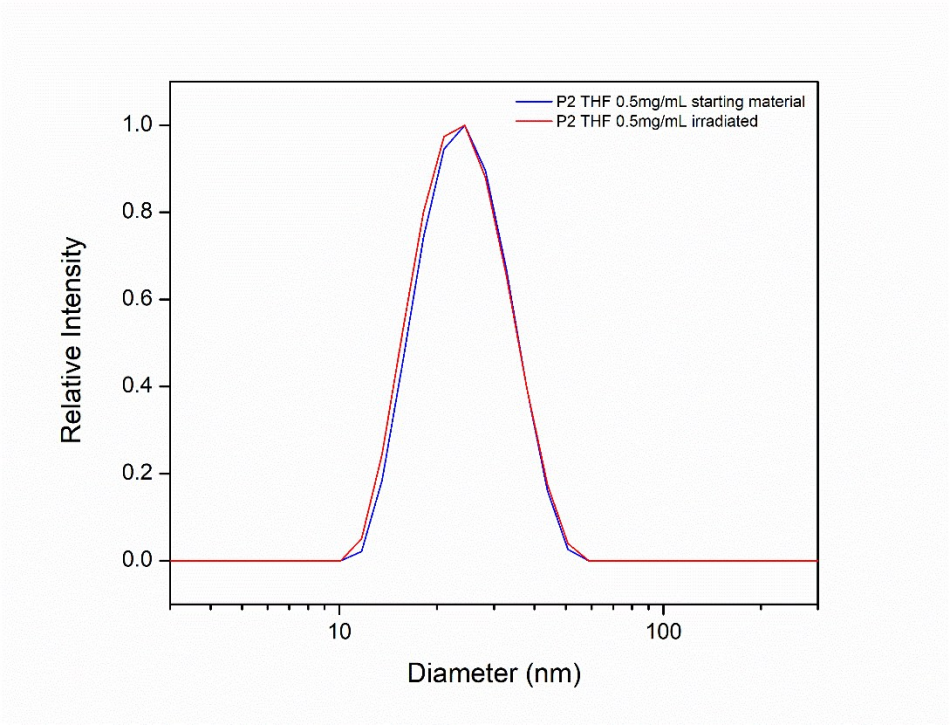

Figure S30. DLS distribution of P2 (blue) and irradiated P2 (red) in THF (*c* = 0.5 mg·mL^{-1})

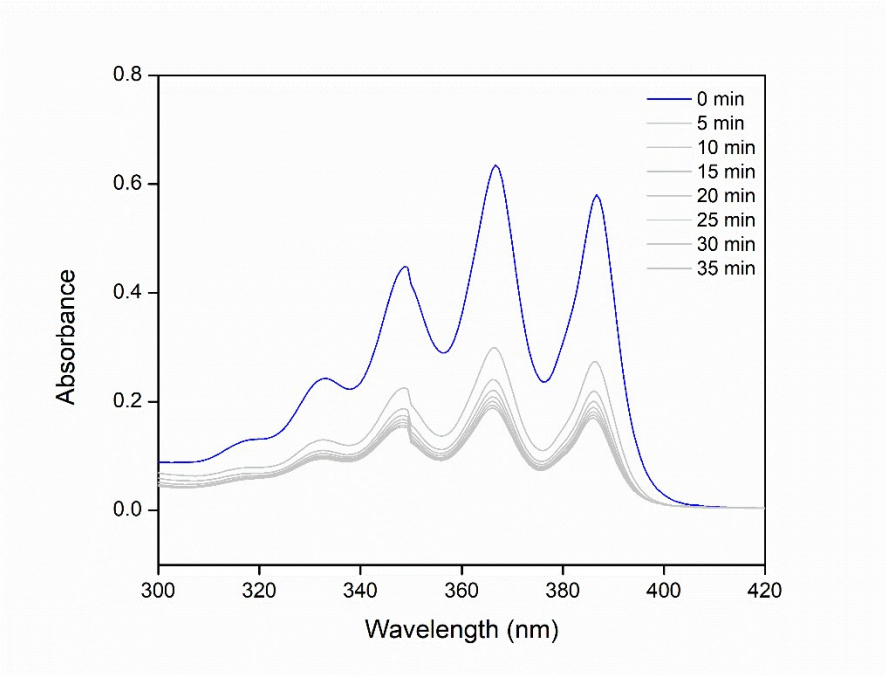

Figure S31. UV-Vis spectra of starting material P2 (blue) and irradiated P2 (grey) in 50/50 (v/v) THF/*n*-hexane (c = 0.5 mg·mL^{-1}) with no prior irradiation

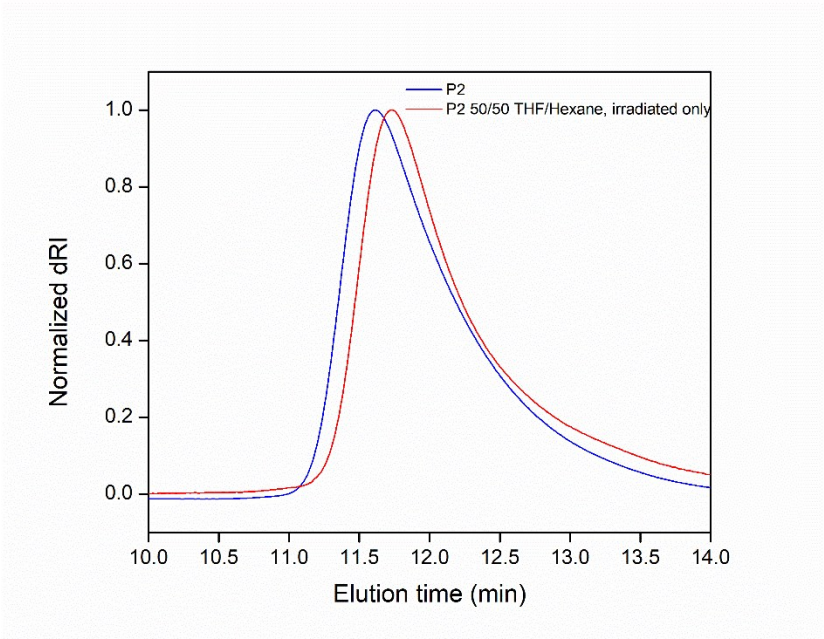

Figure S32. SEC elugram (dRI detector) of pristine P2 (blue) and irradiated P2 (red) in 50/50 (v/v) THF/*n*-hexane (c = 0.5 mg·mL^{-1}) with no prior irradiation

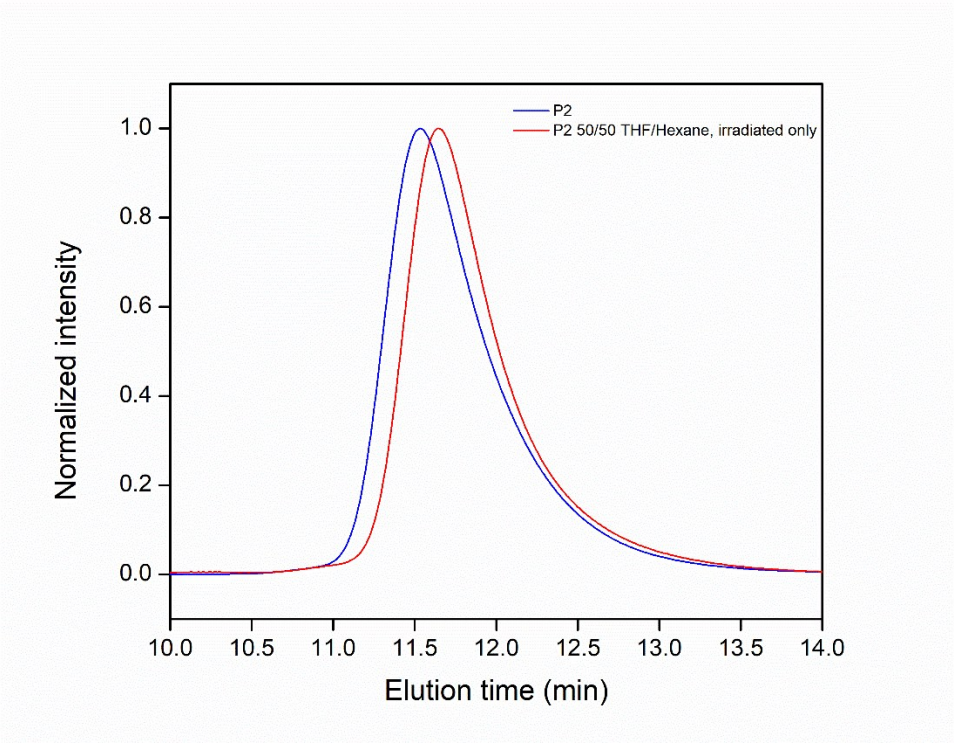

Figure S33. SEC elugram (MALS detector) of pristine P2 (blue) and irradiated P2 (red) in 50/50 (v/v) THF/*n*-hexane(c = 0.5 mg·mL^{-1}) with no prior irradiation

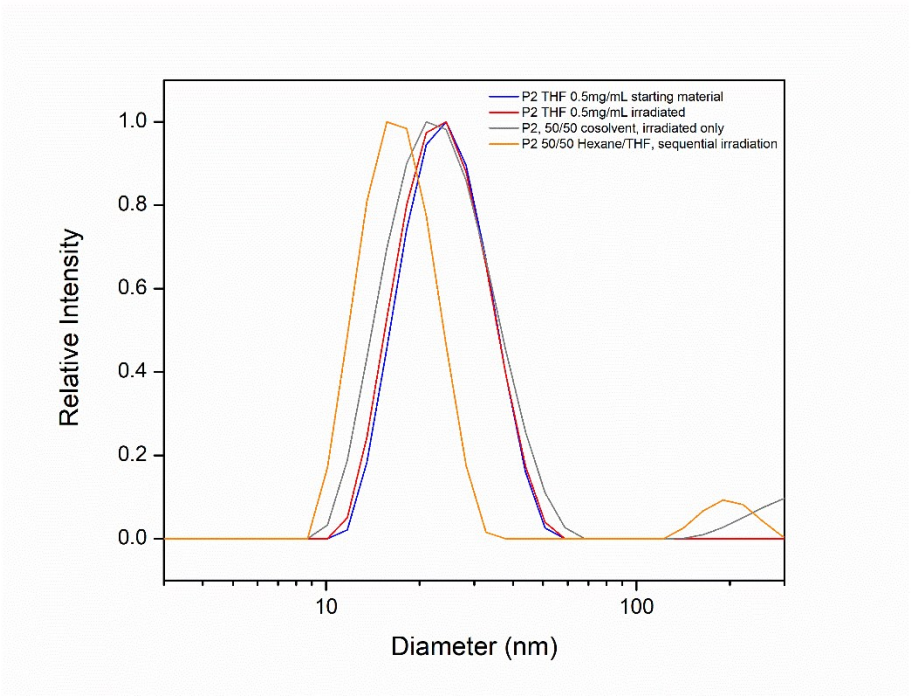

Figure S34. DLS distribution of P2 starting material (*c* = 0.5 mg·mL^{-1}) in THF (blue), P2 post irradiation in THF (red), P2 post irradiation in 50/50 THF/*n*-hexane (v/v) with no prior irradiation (grey), and sequential irradiation of P2 in 50/50 THF/*n*-hexane (v/v) (orange).

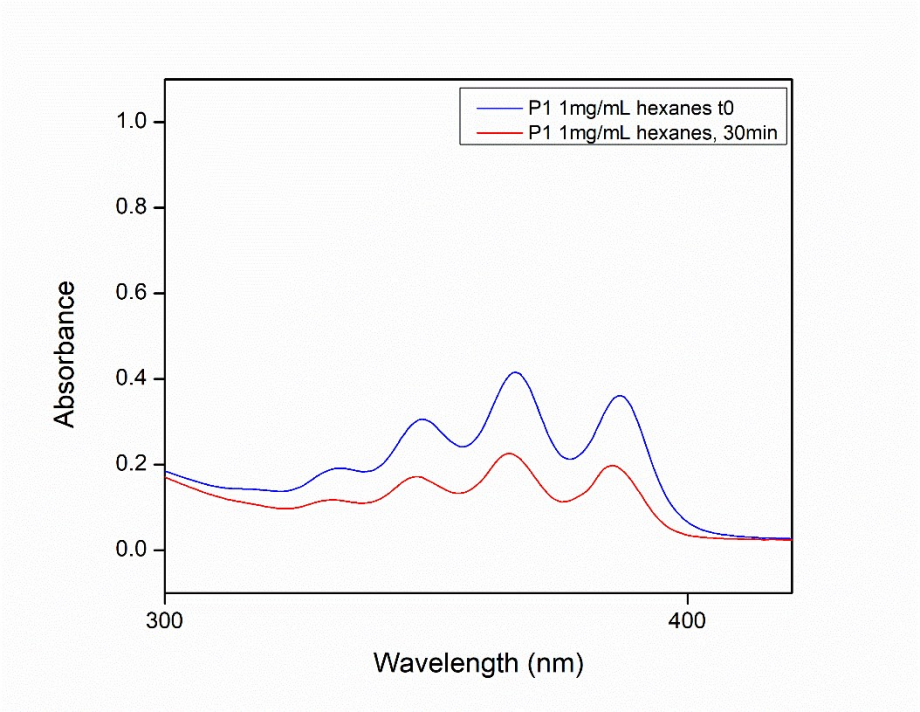

Figure S35. UV-Vis spectra of P1 (blue) and irradiated P1 (red) in *n*-hexanes (c = 1 mg·mL^{-1})

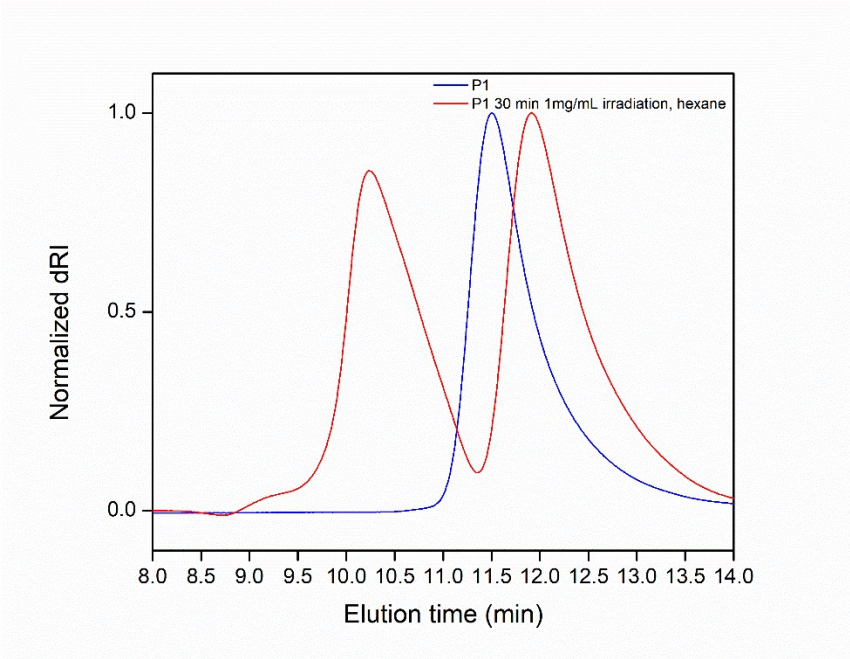

Figure S36. SEC elugram (dRI detector) of pristine P1 (blue) and irradiated P1 (red) in *n*-hexane (c = 1 mg·mL^{-1})

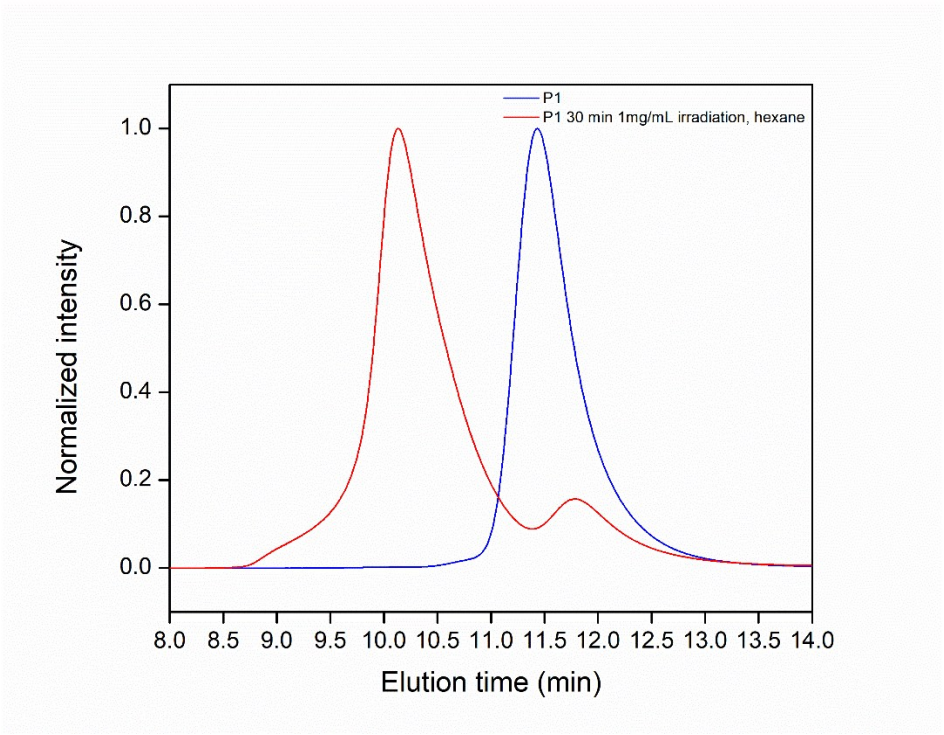

Figure S37. SEC elugram (MALS detector) of pristine P1 (blue) and irradiated P1 (red) in *n*-hexane (c = 1 mg·mL^{-1})

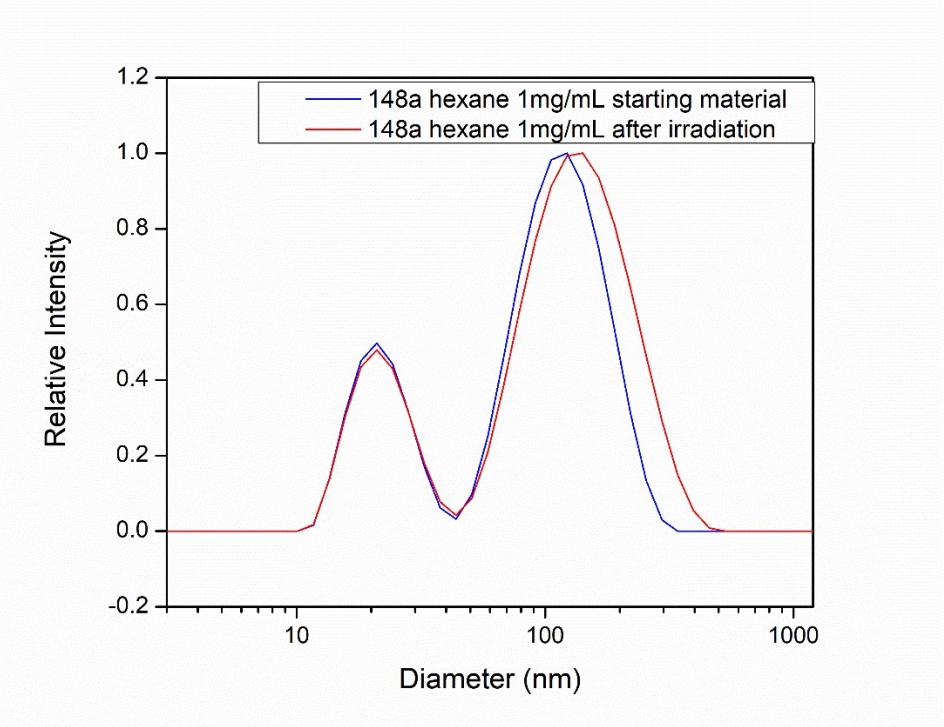

Figure S38. DLS of P1 (blue) and irradiated P1 (red) in *n*-hexanes (*c* = 1 mg·mL^{-1}).

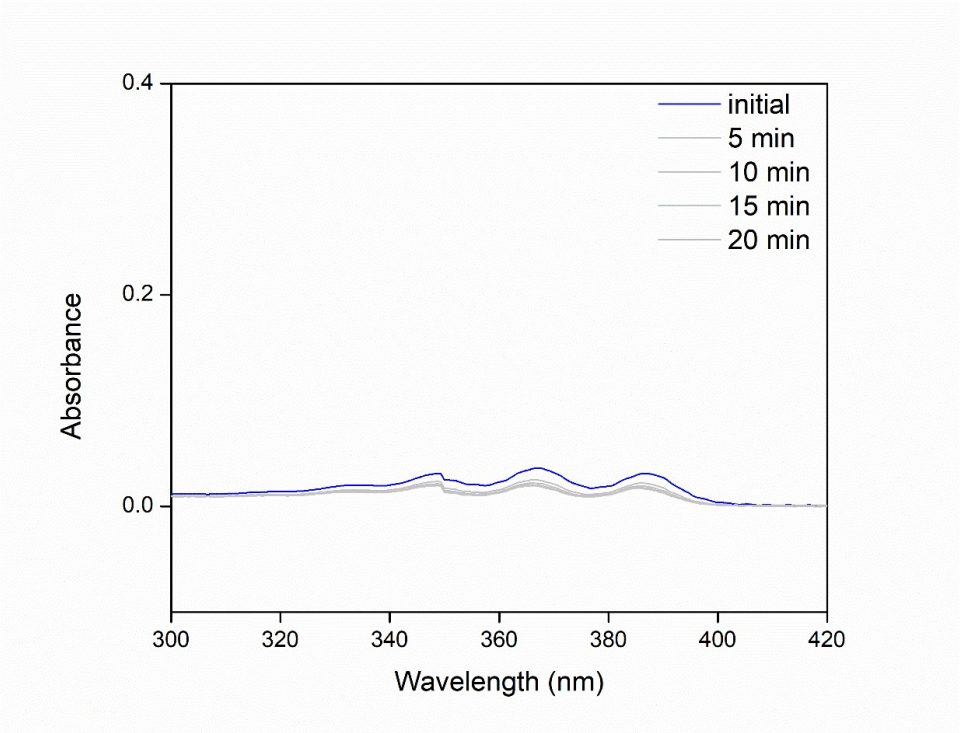

Figure S39. UV-Vis spectra of P1 (blue) and irradiated P1 (grey) in *n*-hexanes (c = 0.1 mg·mL^{-1}). The small bump at 350 nm is due to the instrument switchover.

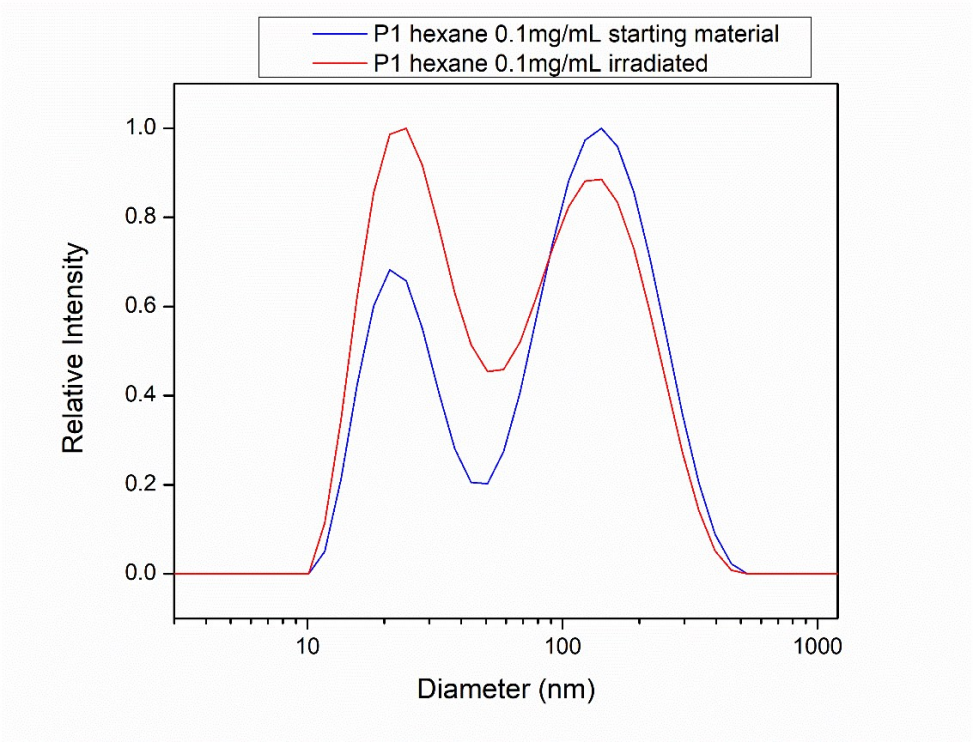

Figure S40. DLS distribution of P1 (blue) and irradiated P1 (red) in *n*-hexane (c = 0.1 mg·mL^{-1})

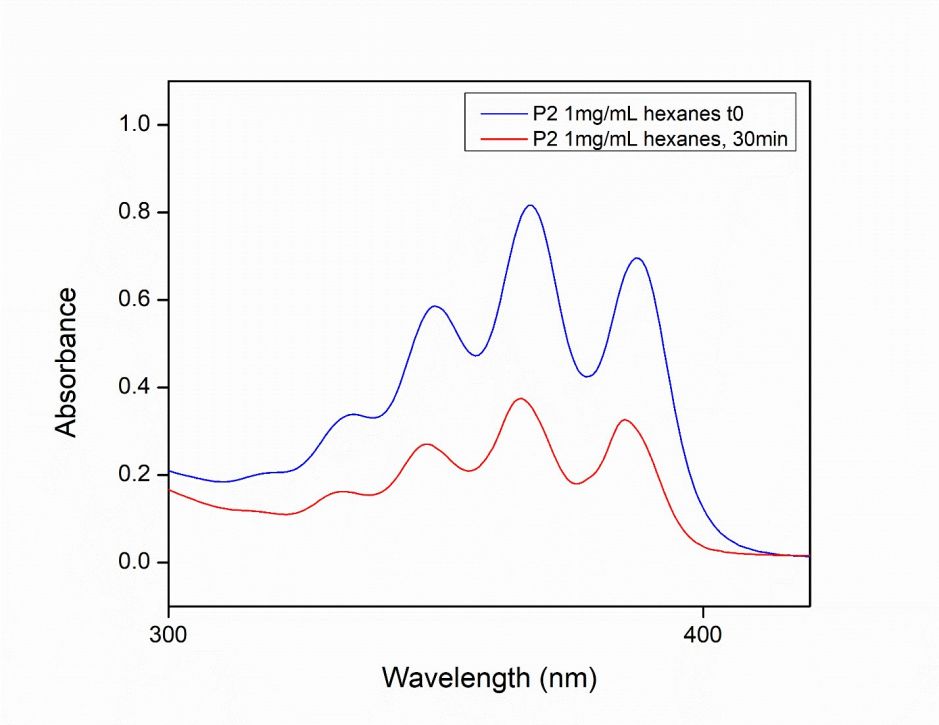

Figure S41. UV-Vis spectra of P2 (blue) and irradiated P2 (red) in *n*-hexanes (c = 1 mg·mL^{-1})

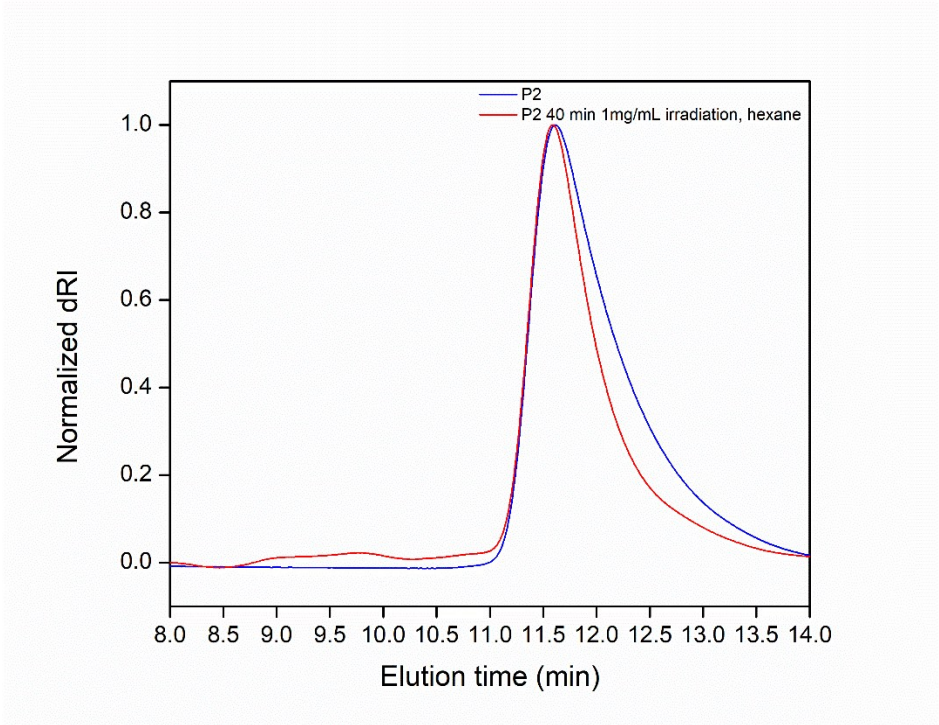

Figure S42. SEC elugram (dRI detector) of pristine P2 (blue) and irradiated P2 (red) in *n*-hexane (c = 1 mg·mL^{-1})

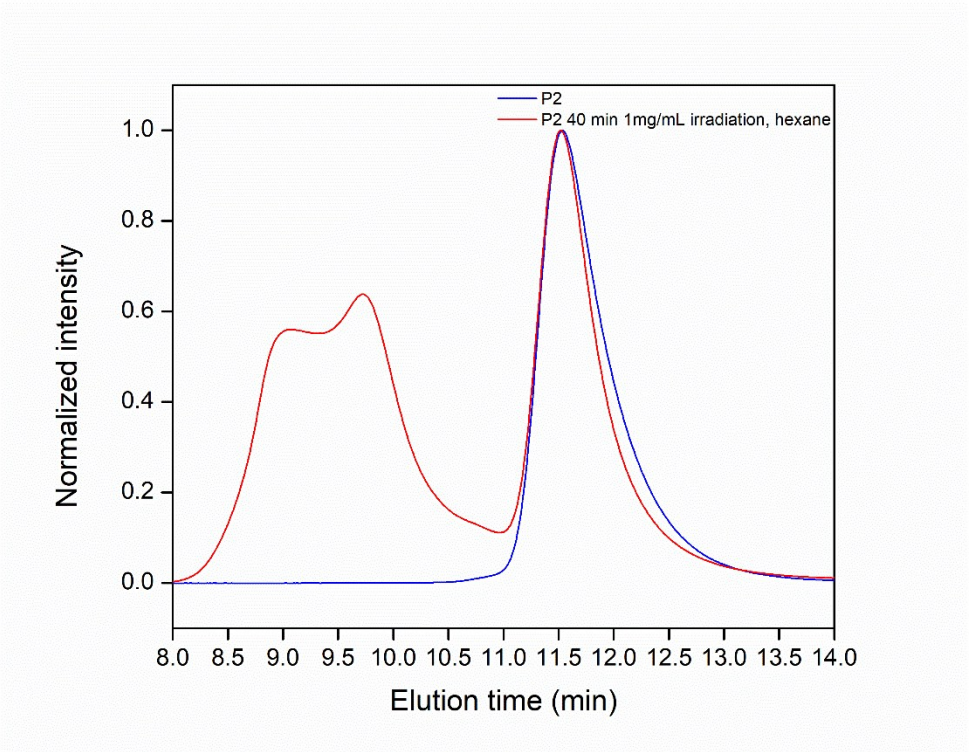

Figure S43. SEC elugram (MALS detector) of pristine P2 (blue) and irradiated P2 (red) in *n*-hexane (*c* = 1 mg·mL^{-1})

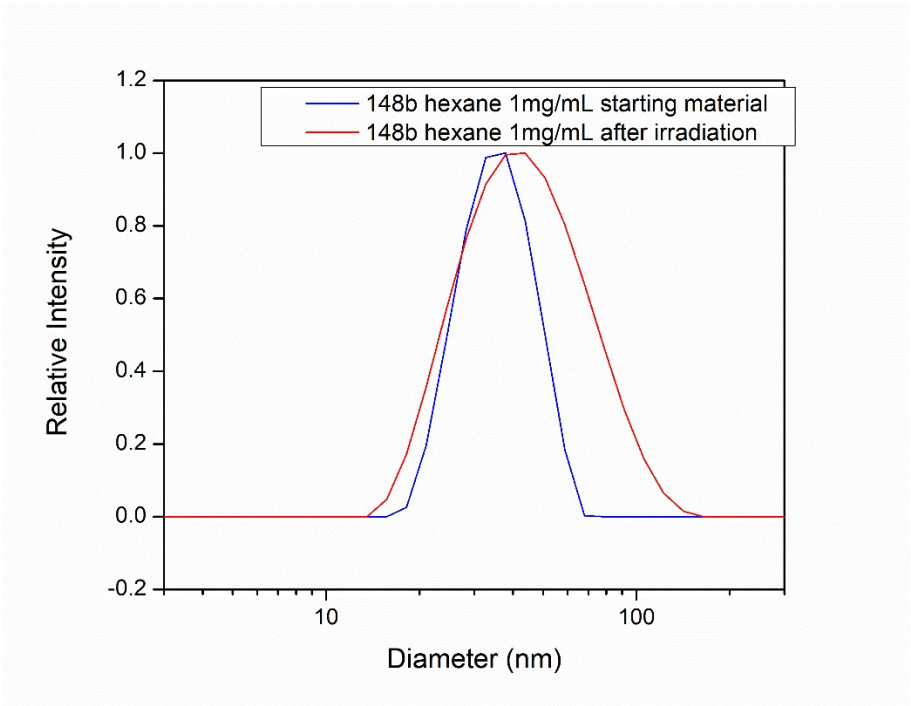

Figure S44. DLS distribution of pristine P2 (blue) and irradiated P2 (red) in *n*-hexanes (c = 1 mg·mL^{-1})

Table S2. DLS data for P1

			Starting		Irradiated	
Solvent System	Concentration ($mg \cdot mL^{-1}$)	Irradiation Time (min)	$R_{H,\ peak\ 1}$ (nm)	$R_{H,\ peak\ 2}$ (nm)	$R_{H,\ peak\ 1}$ (nm)	$R_{H,\ peak\ 2}$ (nm)
THF	1	30	12.95 ± 1.744	-	10.14 ± 0.9525	-
n-hexane	1	30	66.45 ± 3.65	11.64 ± 0.380	77.35 ± 2.3	12.13 ± 0.693
THF	0.5	25	13.76 ± 0.107	-	11.58 ± 0.726	-
n-hexane	0.1	20	66.55 ± 16.94	11.63 ± 1.550	63.2 ± 7.79	13.43 ± 0.587
THF/*n*-hexane	1, then 0.5	55 [30,25]	11.84 ± 0.1425	-	9.88 ± 0.796	-

Table S3. DLS data for P2

			Starting		Irradiated	
Solvent System	Concentration ($mg \cdot mL^{-1}$)	Irradiation Time (min)	$R_{H,\ peak\ 1}$ (nm)	$R_{H,\ peak\ 2}$ (nm)	$R_{H,\ peak\ 1}$ (nm)	$R_{H,\ peak\ 2}$ (nm)
n-hexane	1	40	19.75 ± 1.402	-	23.29 ± 0.277	-
THF	1	40	11.01 ± 1.060	-	9.665 ± 0.617	-
THF	0.5	50	12.70 ± 1.034	-	12.00 ± 0.364	-
THF/*n*-hexane	1, then 0.5	100 [40+60]	13.14 ± 0.425	-	8.315 ± 0.569	-
THF/*n*-hexane	0.5	55	12.70 ± 1.03	-	11.79 ± 0.697	-

Table S4. SEC Data for irradiated P1

Solvent System	Concentration ($mg \cdot mL^{-1}$)	Irradiation time (min)	Peak abscissa (min)	M_n (kg/mol)	M_w (kg/mol)	$Đ$
nonirradiated	-	-	11.503	463	549	1.18
THF	1	30	11.514	415	531	1.27
THF	0.5	25	11.498			
n-hexane[a]	1	30	11.912	495.9	565.1	1.14
THF/*n*-hexane (50/50 v/v)	1, 0.5	55 [30, 25]	11.527	424.6	531.6	1.252

[a] aggregated high molecular weight peaks (not listed) may incur inaccuracy when using the 100% mass recovery assumption for the peak of interest at ~11 minutes

Table S5. SEC data for irradiated P2

Solvent System	Concentration ($mg \cdot mL^{-1}$)	Irradiation time (min)	Peak abscissa (min)	M_n (kg/mol)	M_w (kg/mol)	$Đ$
nonirradiated	-	-	11.613	326	405	1.24
THF	1	40	11.680	325.8	409.7	1.257
THF	0.5	50	11.691	374.2	428.3	1.144
n-hexane[a]	1	40	11.584	491.6	547.5	1.114
THF/*n*-hexane (50/50 v/v)	1, 0.5	100 [40, 60]	11.725	327.3	397.7	1.215
THF/n-hexane (50/50 v/v)	0.5	35	11.728	295.2	377.6	1.279

[a] aggregated high molecular weight peaks (not listed) may incur inaccuracy when using the 100% mass recovery assumption for the peak of interest at ~11 minutes

VIII. References

1 M. S. Sanford, J. a Love and R. H. Grubbs, *Organometallics*, 2001, **20**, 5314–5318.

2 B. Yang, B. A. Abel, C. L. McCormick and R. F. Storey, *Macromolecules*, 2017, **50**, 7458–7467.

3 T. P. Lin, A. B. Chang, H. Y. Chen, A. L. Liberman-Martin, C. M. Bates, M. J. Voegtle, C. A. Bauer and R. H. Grubbs, *J. Am. Chem. Soc.*, 2017, **139**, 3896–3903.